



HHS Public Access

Author manuscript

J Med Chem. Author manuscript; available in PMC 2017 December 22.

Published in final edited form as:

J Med Chem. 2016 December 22; 59(24): 11006–11026. doi:10.1021/acs.jmedchem.6b01183.

Structure-Based Scaffold Repurposing for G Protein-Coupled Receptors: Transformation of Adenosine Derivatives into 5HT_{2B}/5HT_{2C} Serotonin Receptor Antagonists

Dilip K. Tosh[^], Antonella Ciancetta[^], Eugene Warnick, Steven Crane, Zhan-Guo Gao, and Kenneth A. Jacobson^{*}

Molecular Recognition Section, Laboratory of Bioorganic Chemistry, National Institute of Diabetes and Digestive and Kidney Diseases, National Institutes of Health, Bethesda, Maryland 20892 USA.

Abstract

Adenosine derivatives developed to activate adenosine receptors (ARs) revealed μ M activity at serotonin 5HT_{2B} and 5HT_{2C} receptors (5HTRs). We explored the SAR at 5HT₂Rs and modeled receptor interactions in order to optimize affinity and simultaneously reduce AR affinity. Depending on *N*⁶ substitution, small 5'-alkylamide modification maintained 5HT_{2B}R affinity, which was enhanced upon ribose substitution with rigid bicyclo[3.1.0]hexane (North (N)-methanocarba), e.g. *N*⁶-dicyclopropylmethyl 4'-CH₂OH derivative **14** (K_i 11 nM). 5'-Methylamide **23** was 170-fold selective as antagonist for 5HT_{2B}R vs. 5HT_{2C}R. 5'-Methyl **25** and ethyl **26** esters potently antagonized 5HT₂Rs with moderate selectivity in comparison to ARs; related 6-*N,N*-dimethylamino analogue **30** was 5HT₂R-selective. 5' position flexibility of substitution was indicated in 5HT_{2B}R docking. Both 5'-ester and 5'-amide derivatives displayed in vivo *t*_{1/2} of 3–4 h. Thus, we used GPCR modeling to repurpose nucleoside scaffolds in favor of binding at nonpurine receptors, as novel 5HT₂R antagonists, with potential for cardioprotection, liver protection or CNS activity.

Graphical abstract

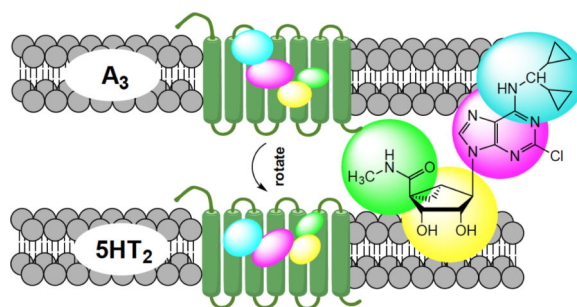
Address correspondence to: Dr. Kenneth A. Jacobson, Laboratory of Bioorganic Chemistry, National Institute of Diabetes and Digestive and Kidney Diseases, NIH, Bethesda, MD 20892-0810 USA. Phone: 301-496-9024. Fax: 301-496-8422.

kajacobs@helix.nih.gov.

[^]equal contribution

Supporting Information Available:

NMR and mass spectra of selected synthesized compounds, results of PDSP screening, MD trajectory Video, additional modeling Figures S1, S2 and S3, Table S1, S2 and S3, 3D coordinates of the starting docking and MD-refined **23**-h5HT_{2B}R complexes, Figure S4 (affinity correlation plot), Figures S5 and S6 (biological data), in vitro ADME measurements. This material is available free of charge via the Internet at <http://pubs.acs.org>.



Keywords

5HT receptor; G protein-coupled receptor; scaffold repurposing; adenosine derivatives; molecular modeling; structure-activity relationship

Introduction

The process of de-risking potential clinical candidate molecules typically involves broad screening at hundreds of off-target activities, consisting of receptors, ion channels, transporters and enzymes.¹ The structure-activity relationship (SAR) of such off-target activities can be analyzed and controlled to either suppress or enhance a secondary activity.² Sometimes a secondary activity within a compound series can become the major focus of a drug discovery program and even lead to an approved drug, as was accomplished for a protease-activated receptor (PAR) 1 antagonist.³ Chemical scaffolds from already approved drugs have been repurposed for new clinical indications, such as kinases drugs that served as the basis of inhibitors of trypanosome replication.⁴ Numerous nucleoside derivatives are approved as pharmaceuticals, indicating that this is a general scaffold that is well-tolerated in vivo.⁵ Other scaffolds have been applied to multiple GPCR families, such as 1,4-dihydropyridines, which have been termed a privileged scaffold, because it can be molded to fit diverse sites.^{6,7}

In the process of examining off-target interactions of nucleoside derivatives that were designed as potent ligands of the A₃ adenosine receptor (AR), we found that occasionally μM affinity was observed at 5HT_{2B} and 5HT_{2C} serotonin receptors (5HT₂Rs). A prototypical A₃AR agonist IB-MECA **10** (Chart 1), containing a ribose 5'-N-methyluronamide group, showed binding K_i values at the 5HT_{2B}R and 5HT_{2C}R of 1.08 and 5.42 μM, respectively.^{8,9} Certain adenine (**1**, **2**) and truncated adenosine derivatives (**3**, **4**) also displayed significant 5HT₂R affinity with K_i < 5 μM.⁹ In the same study, we reported that the substitution of the ribose tetrahydrofuryl ring of adenosine derivatives with a fused bicyclo[3.1.0]hexyl moiety (termed (N)-methanocarba), which maintained a conformation preferred by the A₃AR, was compatible with binding at the 5HT₂Rs. Thus, an otherwise A₃AR-selective agonist **35**, which like **10** has an N⁶-3-halobenzyl group, bound with even greater affinity than riboside **10** at 5HT₂Rs; the K_i values of **35** at 5HT_{2B}R and 5HT_{2C}R were 75 and 122 nM, respectively.⁹ Therefore, these findings provided an opportunity to define more clearly the interaction of nucleosides with 5HT₂Rs and to shift the affinity in favor of this nonpurine receptor activity.

Technology for the discovery of new GPCR ligands is now largely structure-based, with the determination of the X-ray structures of >170 GPCR-ligand complexes.¹⁰ The four ARs belong to the family of rhodopsin-like G protein-coupled receptors (GPCRs). Thirteen of the fourteen 5HTRs, including 5HT_{2B}R and 5HT_{2C}R, are also GPCRs and are located on a different, but closely related branch of rhodopsin-like GPCRs that includes various biogenic amine receptors. The interaction of **35** with the 5HT_{2B}R and 5HT_{2C}R was modeled based on a recently determined X-ray crystallographic structure of the 5HT_{2B}R complex with agonist ergotamine.⁷ Paoletta et al. predicted the binding mode to feature a hydrophobic region deep in the binding site that could accommodate the substituted N⁶-benzyl group of **35**.⁹ Furthermore, a truncated (N)-methanocarba-adenosine derivative containing an N⁶-dicyclopropylmethyl group **4** that acts as a moderately selective agonist of the A₁AR was found to interact at μM concentrations with 5HT₂Rs.⁹ By in silico docking of several adenine and adenosine derivatives to 5HT₂Rs, self-consistent hypotheses for the orientation of the relevant nucleosides in this receptor family were proposed.⁹ Here, we have further explored the SAR of (N)-methanocarba-adenosine derivatives at 5HT_{2B}R and 5HT_{2C}R in an effort to optimize affinity at 5HTRs and simultaneously reduce AR affinity. Thus, we have incorporated and modified structural features of the nucleosides to repurpose the scaffold toward the 5HT-R family.

Selective AR ligands and selective 5HT-R ligands both have varied beneficial activities in disorders of the peripheral and central nervous system (CNS) and in other tissues.^{11,12} 5HT_{2B}R agonist activity is a desirable characteristic in selective serotonin reuptake inhibitors (SSRIs), but peripheral actions at 5HT₂Rs might also have therapeutic potential. 5HT_{2B}R antagonists are sought as agents potentially useful for treating chronic liver and heart disease.^{13,14} Activation of the 5HT_{2B}R by serotonin agonists has been associated with valvulopathy and fibrosis in many organs,^{15–17} 5HT_{2B}R antagonists improved liver function in fibrotic disease models and were described as a “clinically safe” therapy for humans.¹³ In mouse models of coronary function, 5HT_{2B}R antagonists reduced collagen deposits and the resultant right ventricular fibrosis (RVF).¹⁴ A 5HT_{2B}R antagonist is also under development for irritable bowel syndrome.¹⁸ Therefore, the goal of this study is to discover selective 5HT_{2B}R antagonists that might have in vivo activities indicative of the potential for disease treatment. This requires deselecting for 5HT_{2C}R affinity, which is closely associated with 5HT_{2B}R in the present structural series. The combination of potent 5HT_{2B}R antagonist and A₃AR agonist activities¹⁹ in a single molecule might also be beneficial or synergistic for liver protection or cardioprotection.

Results

We have utilized some of the previously reported analogues of adenosine (Table 1, **1–13**, **35–41**) that were characterized as either A₁ or A₃AR-selective agonists,^{20–27} to examine the effects of structural modification on the interaction with 5HT₂Rs. The objectives were to use structural insights to synthesize novel nucleosides (**14–34**, **42**) with enhanced 5HT₂R affinity and at the same time progressively achieve selectivity over the ARs.

The synthesis of the (N)-methanocarba nucleoside analogues was performed as shown in Schemes 1 and 2. The (N)-methanocarba sugar derivative **53** (Scheme 1) was obtained from

D-ribose by a known method.²⁸ Mitsunobu condensation of compound **53** with 2,6-dichloropurine gave the nucleoside derivative **54**, which underwent amination with various amines to give compounds **55–63**. Treatment of TBAF solution with compounds (**55–62**) gave the desilylated compounds **64–71**. The isopropylidene group of compounds (**64–72**) was deprotected with Dowex50 resin to give the nucleoside derivatives **14–21**. Compound **63** was treated with 10% TFA solution at 70 °C to afford compound **22**. The 4'-ethylester derivative **74** (Scheme 2), which obtained from L-ribose by a reported method,²⁹ was converted to nucleoside derivative **75** by a Mitsunobu condensation with 2,6-dichloropurine. Amination of compound **75** with dicyclopropyl amine and *N,N*-dimethyl amine gave compounds **76** and **77**, respectively, which upon acid hydrolysis provided the nucleoside derivatives **26** and **29**. Hydrolysis of ethyl ester group of compounds **26** and **29** with 2N aqueous sodium hydroxide provided the carboxylic acid derivatives **28** and **30**. Coupling of compound **28** with methanol and propanol in the presence of DCC and DMAP gave the ester derivatives **25** and **27**. Treatment of compound **26** and **29** with 40% MeNH₂ solution gave the 5'-methylamide nucleosides **23** and **24**, respectively. Compound **26** was also treated with 1,2-diaminoethane and 1,3-diamino propane to afford the compound **31** and **32**, respectively, which underwent acetylation upon treatment of acetic acid *N*-hydroxysuccinimide ester in the presence of triethylamine to provide acetyl derivatives **33** and **34**.

The binding assays at diverse receptors and transporters, other than ARs, were performed at the Psychoactive Drug Screening Program (PDSP) at the University of North Carolina under the direction of Bryan L. Roth.¹ Initially a concentration of 10 μM was used to probe binding at diverse sites, and compounds that achieved >50% inhibition at this concentration were analyzed with full curves to determine K_i values. We have focused on the 5HT_{2B}R and 5HT_{2C}R, because none of the compounds tested showed significant interaction (>50% inhibition at 10 μM) in binding assays at other 5HTRs: 5HT_{1A}, 5HT_{1B}, 5HT_{1D}, 5HT_{1E}, 5HT₄, 5HT₆ and 5HT₇. Affinity at the 5HT_{2A}R, which is related in sequence to 5HT_{2B}R and 5HT_{2C}R, was also consistently low (K_i > 10 μM) or absent; when <50% inhibition was noted at any of the 5HT₂Rs, the % values at are provided in the table. However, one compound displayed measurable affinity at the 5HT₃R, e.g. truncated nucleoside **3**, K_i 3.26 ± 0.54 μM (n = 3), and compound **30** bound weakly to the 5HT_{5A}R.

Binding at the 5HT_{2B}R and 5HT_{2C}R was performed using standard high affinity radioligands, [³H]**43** and [³H]**44**, respectively. As we reported previously, adenine derivatives **1** and **2**, lacking *N*⁹ substitution, or with a 2',3'-dihydroxy-bicyclo[3.1.0]hexyl substitution of ribose, i.e. **3** and **4**, bound to the 5HT_{2B}R with μM affinity.⁹ Appending the adenine C2 substitution with a rigid arylethynyl group in **2** maintained affinity at the 5HT_{2B}R, but eliminated μM affinity at the 5HT_{2C}R that was observed with compounds **1**, **3** and **4**. Ribonucleosides **5–9**, known AR agonists that display varied AR selectivities, were found to be inactive at 5HT₂Rs. Compound **5** is often taken to closely approximate the pharmacology of adenosine itself; thus, it is unlikely that endogenous adenosine would be interacting with 5HT₂Rs in situ. Depending on *N*⁶-substitution, appending a 9-ribose moiety with a small alkyl amide modification at the 5' position was tolerated at the 5HT_{2B}R, as with compounds **10** and **11**. Changing C2-H **10** to C2-Cl **11** in the ribose series did not have

a major effect on the 5HT₂R affinity; both of those A₃AR-selective agonists are in current clinical trials.³⁰

The SAR of (N)-methanocarba derivatives **12** – **42** was analyzed in detail. In the 4'-CH₂OH series **12** – **22**, a slight increase of 5HT₂R affinity was observed with introduction of an N⁶-methyl group on the exocyclic amine (as in previously reported (N)-methanocarba nucleosides **13** vs. **12**). Enhancement of 5HT₂R affinity was observed upon introduction of a rigid (N)-methanocarba moiety, compared to ribose, in analogues containing a 4'-hydroxymethyl group (as in **12** vs. **5**; **14** vs. **6**, in which the C2 substitution also changes). Notably, N⁶-dicyclopropylmethyl 4'-CH₂OH derivative **14** containing a (N)-methanocarba substitution displayed a potent K_i value of 11 nM at the 5HT_{2B}R with slight (8-fold) selectivity vs. 5HT_{2C}R (*P* < 0.05, unpaired t-test). Consequently, analogues of **14** with slight modifications of the N⁶-dicyclopropylmethyl group and defined stereochemistry (compounds **15**–**21**) were evaluated in an attempt to tune the pharmacological properties. Cyclopropyl was changed to ethyl, isopropyl or cyclobutyl in an effort to enhance 5HT_{2B}R affinity or selectivity. Thus, pairs of diastereomeric nucleosides differing in the chirality of the C α group at N⁶ were compared. In comparing N⁶-dicyclopropylmethyl derivative **14** with *R*-isomers **16**, **18**, and **21** and with *S*-isomers **17**, **19**, and **20**, there was no consistent preference for a particular stereoisomer, and all of these variations of **14** moderately reduced the 5HT_{2B}R affinity. Also, the N⁶-achiral derivative **15** was most reduced in 5HT₂R affinity compared to **14**. Among these chiral N⁶ derivatives of **14**, *S*-isomer **20** was the most potent at the 5HT_{2B}R (K_i 34 nM), and *R*-isomer **18** was the most potent at the 5HT_{2C}R (K_i 190 nM).

5'-Carbonyl group modifications had variable effects on A₃AR affinity in comparison to the corresponding 4'-CH₂OH. The 5'-methylamide derivative **23**, related to N⁶-dicyclopropylmethyl analogue **14**, was 12-fold selective in binding for 5HT_{2B}R vs. 5HT_{2C}R (*P* < 0.05, unpaired t-test). However, the same 5'-methylamide in the (N)-methanocarba series generally resulted in small decreases in 5HT_{2B}R affinity (K_i 23 nM, **23** vs. 11 nM, **14**) and 5HT_{2C}R affinity (K_i 269 nM, **23** vs. 84 nM, **14**). 5'-Methyl ester **25** and 5'-ethyl ester **26** derivatives were particularly potent and selective at the 5HT₂Rs (15–19 nM at 5HT_{2B}R) with only intermediate affinity at the ARs (roughly μ M). Compound **25** was 6-fold selective for the 5HT_{2B}R compared to 5HT_{2C}R (*P* < 0.05, unpaired t-test),

Representative inhibition curves are shown for 5'-methyl ester **25** (Figure 1), which bound to the 5HT_{2B}R as potently as the reference compound **49**. The corresponding 5'-propyl ester **27** and 5'-carboxylic acid derivative **28** were less potent at the 5HT₂Rs than the methyl and ethyl esters.

For comparison, we include affinities at the human A₁AR, A_{2A}AR and A₃AR, often from archival data (Table 1).^{21–26} Selected newly synthesized structures were assayed at 10 μ M at the A_{2A}AR, which is disfavored in binding of (N)-methanocarba adenosines in general. We did not include affinity at the human A_{2B}AR, because we already established that in the (N)-methanocarba series, especially those containing compounds C2 substitution, the affinities tend to be much lower at that subtype than at the other AR subtypes.²⁵ (N)-Methanocarba 4'-hydroxymethyl **14** and 5'-methylamide **23** derivatives were more potent at the A₃AR

than the corresponding 5'-alkyl esters **25** – **27**. However, **14** was most potent at the A₁AR with a K_i value of 39 nM. The affinity at the A₁AR and A₃AR of the diastereomeric nucleosides **16** – **21** was significantly reduced (typically by 20- to 30-fold) compared to **14**. Similarly, in a previous modeling study of the 4'-truncated equivalents of compounds **14** – **21**,²² any deviation from the N⁶-dicyclopropylmethyl group reduced both A₁AR and A₃AR affinity. Furthermore, **25** was significantly more potent at 5HT_{2B}R than at A₁AR (23-fold) and A₃AR (40-fold) ($P < 0.05$, one-way ANOVA with post-hoc test). Functional assays of A₁AR-mediated inhibition of cAMP formation²² showed that **14** and **26** were full agonists, with maximal efficacy (at 10 μM) of 104±4% and 89±3% of N⁶-cyclopentyladenosine (1 μM). In a functional assay of A₃AR-mediated inhibition of cAMP formation (n=3),²² esters **25** and **26** were partial agonists (at 10 μM) with maximal efficacy of 41.4±2.8% and 26.3±6.1%, respectively, compared to **48** set at 100%, and amide **23** was a full agonist (96.7±1.0%).

All of the previous analogues mentioned up to this point contained either an exocyclic NH₂ group or a monosubstituted NH. The effects of di-methyl substitution of the N⁶ group was examined in the following 2-Cl analogues: 4'-hydroxymethyl **22**, 5'-methylamide **24**, 5'-ethyl ester **29** and 5'-carboxylic acid **30** derivatives. The 4'-CH₂OH analogue **22** displayed K_i values of 5–8 μM at 5HT_{2B}R and 5HT_{2C}R and ~2.5 μM at the A₃AR. The corresponding 5'-CONH-Me analogue **24** displayed only slightly improved μM affinity at 5HT_{2B}R, 5HT_{2C}R and A₃AR. However, the corresponding 5'-ethyl ester analogue **29** displayed K_i values of 671 nM at 5HT_{2B}R and 1.35 μM at 5HT_{2C}R with no measurable affinity at the A₃AR. Thus, N⁶-dimethyl analogue **29** was 5HT_{2R}-selective in binding assays. 5'-Carboxylate derivatives **28** and **30** displayed roughly μM affinity at the 5HT_{2B}R, 5HT_{2C}R and A₃AR.

In order to reduce AR affinity while further enhancing 5HT_{2R} affinity, we examined in detail the molecular modeling of these GPCRs. The docking of nucleoside derivatives at the 5HT_{2B}R by Paoletta et al. proposed two hypothetical binding modes depending on substituent groups.⁹ The most general docking mode, applicable to all nucleosides examined, proposed that a nonpolar N⁶ group, i.e. a 3-chlorobenzyl group in **35**, was anchored the analogues in a deep hydrophobic region.² This mode would allow the ribose moiety access to the exofacial side of the receptor and therefore might provide greater flexibility of substitution. An alternative mode of 5HT_{2B}R docking, which was very similar to the position of related adenosine derivatives in ARs with the ribose moiety facing downward in a deep hydrophilic region, was possible only in the absence of an extended C2 substituent. We proceeded initially assuming the first predicted binding mode (above), leading to the hypothesis that the more external ribose moiety (or (N)-methanocarpa moiety) would have considerable freedom of substitution in binding to the 5HT_{2B}R. In order to design analogues that might lack interaction with ARs, we referred to our previous studies of the modification of 5'-amide derivatives in the adenosine (9-riboside) series.³¹ It was noted that 5'-N-2-aminoethyl and 5'-N-3-aminopropyl amides in the ribose series were of greatly reduced AR affinity. Therefore, we prepared compounds **31** and **32**, which are 5'-N-(aminoalkyl)amide derivatives containing the preferred N⁶-dicyclopropylmethyl group to test if the interaction with the 5HT_{2R}s would be maintained. In fact, these two compounds

bound with moderate affinity at 5HT_{2B}R and 5HT_{2C}R, with a preference for the 5HT_{2C}R (both displayed K_i values of ~140 nM). Moreover, as predicted by receptor docking modes, compounds **31** and **32** were selective for the 5HT₂Rs in comparison to ARs. Therefore, we added two more analogues **33** and **34**, which were the *N*-acetylation products of **31** and **32** and that displayed roughly μM or sub-μM affinity in 5HT₂Rs and K_i values of ~1.7–2.0 μM at the A₃AR. Evidently, there is a freedom of substitution at the 5HT₂Rs of this extended functionalized chain attached at the 5'-CO position, consistent with modeling predictions that indicate the ribose moiety to be pointing toward the extracellular medium. However, in AR docking, based on the X-ray structures of nucleoside-bound A_{2A}ARs, the ribose binding subpocket and the region around the 5' position are more sterically limited. Curiously, compound **33** displayed a K_i value of 0.40 μM at the A₁AR, which was more potent than other members of the extended 5'-amide series.

Effects on 5HT₂R affinity of extensions at the C2 position were compared. Compound **35** has been studied as a potent A₃AR agonist in an inflammation model.³⁰ Although it displayed substantial affinity at 5HT₂Rs, **35** was nevertheless 260-fold selective for A₃AR vs. 5HT_{2B}R. Other (N)-methanocarba derivatives with extended C2 substituents **36–41**, which were already reported as particularly potent and selective at the A₃AR,^{20,22–26} displayed at best μM affinity at 5HT₂Rs, e.g. **37**, **38**, and **41**. Thus, the approach of C2 extension that we have taken in recent SAR studies to enhance A₃AR selectivity generally precluded activity at 5HTRs. The dialkylation of the exocyclic amine of **42** slightly increased affinity at the 5HT_{2C}R with an accompanying 34-fold reduction of A₃AR affinity (**39** vs. **42**).

Functional assays indicated antagonist activity of **14** and **26** at 5HT_{2B/C}Rs, similar to our previous report with adenine/adenosine derivatives that are moderately potent 5HT₂R ligands.⁹ Compounds **1** and **35** were previously found to be antagonists of the 5HT_{2B}R and 5HT_{2C}R, with functional IC₅₀ values at 5HT_{2B}R of 0.89 and 3.26 μM, respectively.⁹ Here, K_i values in fully antagonizing receptor activation by serotonin at 5HT_{2B}R and 5HT_{2C}R were determined (Figures 1C,D), respectively, for compounds (n=): **14**, 22.3±4.0 nM (2) and 337±27 nM (2); **23**, 4.4±2.6 nM (4) and 752±431 nM (3); **25**, 3.2±1.9 nM (4) and 4.1±1.6 nM (4); **26**, 1.8±0.7 nM (3) and 3.9±2.9 nM (3). Thus, 5'-methamide **23** displayed 170-fold selectivity at 5HT_{2B}R. Compounds **14**, **23**, **25**, and **26** at 10 μM had no appreciable agonist or partial agonist activity at 5HT_{2B}R and 5HT_{2C}R and no activity as agonist or antagonist at 5HT_{2A}R (Figure 2, Figure S6, Supporting Information). Therefore, within the 5HT₂Rs, all four derivatives were potent antagonists at two subtypes, and 5HT_{2B}R functional selectivity was observed for amide derivative **23** (Figure S7, Supporting information). The ligand efficiency (LE) in 5HT_{2B}R binding for four compounds was: **14**, 0.41; **23**, 0.37; **25**, 0.37; **26**, 0.37.

Two representative *N*⁶-dicyclopropylmethyl derivatives **23** and **25** that differed only at the 5' position were examined for ADME and toxicological parameters (Table 2, Supporting Information). 5'-Methylamide **23** and 5'-methyl ester **25** demonstrated ~100% stability in human plasma over 2 h, and 87% **23** and 94% **25** remained after 1 h exposure to human liver microsomes with cofactor present. Both compounds lacked inhibition of cytochrome P450 enzymes (Table 2) and were found to be relatively non-toxic to HepG2 liver cells (growth

inhibition <30% at 30 μM). Their stability at pH 6.5 was high, with 97% of each compound remaining after 2 h in simulated intestinal fluid). However, the stability in simulated gastric fluid at pH 1.6 showed only ~50% of each compound remaining after 2 h. The reduced acid stability is likely common to compounds containing a N^6 -dicyclopropylmethyl group. **23** was moderately permeable in CACO-2 cells with evidence of efflux (A-to-B $P_{\text{app}} = 4.73 \times 10^{-6}$ cm/sec; efflux ratio = 11.7), while **25** was highly permeable with no significant efflux (A-to-B $P_{\text{app}} = 18.5 \times 10^{-6}$ cm/sec; efflux ratio = 1.67). The half-life following intravenous administration (1.0 mg/kg) in male Sprague-Dawley rats was 2.89 ± 0.67 h for **23** and 3.56 ± 0.32 h for **25** (mean \pm SEM, $n = 3$). Thus, the ester group of **25** was not subject to rapid hydrolysis, probably due to the steric hindrance of the tertiary 4'-carbon. Compound **23** ($C_0 = 1070 \pm 30$ ng/mL; $V_{\text{dss}} = 3.16 \pm 0.41$ L/kg) displayed better pharmacokinetic exposure than **25** ($C_0 = 349 \pm 7$ ng/mL; $V_{\text{dss}} = 4.62 \pm 0.18$ L/kg).

A few other off-target activities ($K_i < 10$ μM) at receptors and ion channels determined by the PDSP that are not already reported were detected (Figure S5, Supporting Information). For example, riboside derivative **9** showed only two such interactions (K_i at σ_1 and σ_2 receptors, 4.1 and 1.4 μM , respectively). Compounds **13** and **42** displayed K_i values at the σ_2 receptor of 2.22 ± 0.88 and 7.3 μM , respectively. Compound **14** inhibited binding at the dopamine transporter (K_i 4.8 μM) and compounds **26** and **27** at the translocator protein (TSPO, K_i 2.1 μM and 2.2 μM , respectively). There were no such interactions with other closely related GPCR families: muscarinic cholinergic, α - and β - adrenergic, dopaminergic or histaminergic receptors.

Molecular Modeling

We performed docking and MD simulations to explain the observed binding data by focusing on the h5HT_{2B}R. The available X-ray structure of the receptor in complex with the biased agonist ergotamine (ERG) features signatures of both active and inactive states,³² thus entailing potential limitations in using this structure to elucidate the binding of antagonists. We therefore built a homology model for the native h5HT_{2B}R using the ERG-h5HT_{2B}R X-ray structure as template,³² docked a selected compound by means of induced fit docking (IFD), and refined the obtained binding pose with 30 ns of membrane MD simulations.

Induced Fit Docking—For our modeling analysis, we focused on the N^6 -dicyclopropylmethyl 5'-methylamide derivative **23**, which is 12-fold selective in binding at the h5HT_{2B}R in comparison to the h5HT_{2C}R. The compound was docked into the h5HT_{2B}R homology model by means of IFD (docking score -8.265 kcal/mol). As depicted in Figure 3A, the ligand lies perpendicular to the membrane plane with the pseudo-sugar moiety pointing toward the extracellular side in an orientation similar to the most general (ribose-up) binding mode previously described.⁹ A network of hydrogen bonds and extended hydrophobic contacts (Figure 3A) anchor the ligand to the upper part of TM2, TM3 and TM7, and to the downstream region of the second extracellular loop (EL2). The NH group of the amide moiety in 5' and the secondary amino group (N^6) act as H-bond donors to the backbone of Cys207^{EL2} of the conserved disulfide bridge and the sidechain of the conserved Asp135^{3,32} residue, respectively. The 2' and 3' OH groups of the pseudo-sugar moiety

establish H-bond interactions with the sidechains of Gln359^{7,32}, Glu363^{7,36}, and Thr114^{2,64}. The *N*⁶-dicyclopropylmethyl moiety engages in extended hydrophobic contacts with residues located in TM3 (Leu132 and Val136), TM6 (Trp337 and Phe340), TM7 (Val366 and Tyr370), and at the interface between EL2 and TM5 (Leu209 and Phe217). The methyl group of the 5'-methylamide points toward TM3 and establishes hydrophobic contacts with Trp121^{EL1}, Trp131^{3,28}, and the sidechain of Cys207^{EL2}. The (N)-methanocarba ring faces the extracellular side and engages in hydrophobic contacts with Val208^{EL2}.

MD simulations—The above-described binding mode of **23** was subjected to 30 ns of all-atom MD simulations. The visualization of the trajectory (Video S1) along with the Interaction Energy (IE) profile (Lower right panel in Video S1 and Figure S1) showed that the interaction network did not persist when water molecules were allowed to diffuse into the membrane-embedded system. Indeed, after a few ns, a flip of the glycosidic bond (Video S1) triggered the ligand to move deeper in the binding site and to establish an extended network of H-bond interactions with the conserved Asp135^{3,32} and Tyr370^{7,43} through the interplay of water molecules. The pseudoglycosidic bond angle was -117.2° for the docked compound (*anti*) and 12.7° for the final structure after MD (*syn*). In the other two trajectories (data not shown), the flip of the glycosidic bond was assisted by an H-bond interaction between the side chain of Glu363^{7,36} and the 5'-methylamide moiety. As this residue occurs as Asn^{7,36} in the h5HT_{2C}R, we believe that this transient interaction might assist the ligand while approaching the binding site and therefore might account for the h5HT_{2B}R selectivity of the 5'-methylamide with respect to 5'-alkylester groups. The new placement of the ligand (Figure 3B) - with the adenine core lying almost parallel to the membrane plane and the *N*⁶-dicyclopropylmethyl moiety pointing toward TM5 and TM6 - persisted for the rest of the trajectory and was stabilized by extended water-mediate H-bond interactions. The binding mode proposed by the MD analysis (Figure 3B) features a π - π stacking interaction between the adenine core and Phe340^{6,51} and nine tightly bound water molecules (*w1-w9*) mediating the ligand-protein H-bond interactions: *w1* (highlighted in yellow) anchors the 5'-carbonyl group to the sidechain of Gln359^{7,32} (acting as H-bond donor) and the backbone of Leu209^{EL2} (acting as H-bond acceptor); *w2* and *w3* (highlighted in magenta) connect the 2' OH group of the pseudo-sugar moiety to conserved Asp135^{3,32} and Tyr370^{7,43}; *w4* and *w5* (highlighted in green) bridge the backbone of Cys207 to the sidechain of the conserved Asp135^{3,32} through the interplay of the 3' OH group; *w6* (highlighted in purple) mediates the H-bond interaction between the sidechain of Ser139^{3,39} and the *N*⁶ amine; *w7-w9* (highlighted in cyan) connect the N3 nitrogen atom of the adenine core to the sidechains of the conserved Asp135^{3,32} and Asn344^{6,55} residues. This putative binding mode agrees with the flexibility of substitution at the 5' position of the pseudo-sugar moiety as well as with the intolerance of bulkier groups at the adenine C2 position (pointing toward TM6). Indeed, active compounds bearing different groups at the 5' position (**14**: hydroxy; **25**: methyl ester; **26**: ethyl ester; **27**: propyl ester, Figure 4A–D) as well as the *N*⁶-3-chlorobenzyl 5'-methylamide derivative **35** (data not shown) docked to this receptor conformation with good scores (Table S1) by maintaining the above describe interaction pattern and by retaining water molecules. Notably, as reported in Table S1, we were able to dock the compounds using also the XP scoring function, which is known to

require a greater ligand-receptor shape complementarity, thus further emphasizing the feasibility of this interaction network.

As emerged from this analysis, all of the ligand-receptor interactions, except the H-bond network mediated by *w1* and a hydrophobic contact with Met218^{5,39} (transparent surface on the right in Figure 3B), involve highly conserved residues. Nonetheless, we believe that these two interactions might account for the greater affinity of **23** for the h5HT_{2B}R. Indeed, the h5HT_{2C}R features a Glu residue (whose sidechain that cannot act as H-bond donor) in place of Gln^{7,32} and a shorter EL2. While the Glu^{7,32} side chain would not enable the H-bond network as mediated by *w1* in the h5HT_{2B}R, the shorter EL2 is expected to affect the three-dimensional arrangement of the downstream loop region as well as of the extracellular tip of TM5 – where Leu 209 and Met^{5,39} (occurring as Val^{5,39} in the h5HT_{2C}R), respectively, are located.

Concerning the activity at the hA₁ and hA₃ARs exhibited by 5'-methylamide derivatives, we expect binding modes similar to the previously discussed poses of (N)-methanocarba adenosines^{21,33} envisaging the placement of the scaffold perpendicular to the membrane plane with the pseudo-sugar pointing toward the intracellular side. In this binding mode, the C2' and C3' OH groups interact with the sidechains of the conserved His^{7,43} and Ser^{7,42}, respectively, and the NH group of the 5'-methylamide engages in an H-bond interaction with Thr^{3,36}.

Analysis of Receptor Structures—The overlay between the starting docking structure and the MD-refined complex (Figure S2A, alignment base on alpha carbon atoms of TM domains) shows that the largest structural rearrangements in the protein occurred in TM5, TM6, and TM7. In the final **23**-h5HT_{2B}R structure (cyan ribbons in Figure S2A), the bulge in TM5 – that protruded into the binding site in the initial structure (magenta ribbons in Figure S2A) – was pushed outward by the *N*⁶-dicyclopropylmethyl moiety of the ligand, the intracellular tip of TM6 moved toward the TM bundle, and a disruption of the alpha helix structure in TM7 (residues 372 to 374) occurred. All these structural rearrangements are compatible with a transition from an active-like to an inactive protein structure, as emerged by the comparison between the β₂-adrenergic active³⁴ and inactive³⁵ structures. Moreover, the average distances of the sidechains of Phe^{6,41} and Phe^{6,44} with respect to TM5 ($d(C_4\text{-Phe}^{6,44}\text{-C}_\alpha\text{-Pro}^{5,50}) = 12.8 \text{ \AA}$; $d(C_4\text{-Phe}^{6,41}\text{-C}_\alpha\text{-Met}^{5,54}) = 9.8 \text{ \AA}$) and the sidechain of Tyr^{7,53} oriented toward TM3 further suggest that the final receptor structure is in the inactive state.^{36,37} In addition, the average density of water molecules calculated during the trajectory (Figure S2B) highlighted the presence of the previously hypothesized³⁶ hydrophobic connector that hampers the entrance of water molecules.

We also performed the check of the “inactive signatures”³⁷ by comparing the results with MD simulations of the apo receptor. Surprisingly, the ionic lock between Arg^{3,50} and Glu^{6,30} persisted in the h5HT_{2B}R-apo structure but not in the ligand-bound structure (Figure S3A, Supporting Information). Indeed, in the **23**-h5HT_{2B}R complex, Arg^{3,50} establishes a persistent H-bond interaction with the sidechain of Tyr^{7,53} of the conserved NPxxY motif (Figure S3B). In both structures, the salt bridge between Asp^{3,49} and Arg^{3,50} (conserved DRY motif, Figure S3C) is not present because Asp^{3,49} faces TM4 and establishes a salt

bridge with Lys^{4.45} (Figure S3D). According to structure-based sequence alignments,³⁸ Lys^{4.45} is a not conserved residue present only in the h5HT_{2A}R, h5HT_{2B}R, h5HT_{2C}R and human histamine H₃R. Indeed, other biogenic amine receptors as well as nucleotide receptors feature a positively charged residue (Lys or Arg) in the 4.41, 4.43 or 4.44 position (Table S2). Moreover, in the h5HT_{2B}R structure experimentally determined through serial femtosecond crystallography,³⁹ a salt bridge between Glu^{3.60} and the non-conserved Lys^{5.68} was found. This provided further evidence of the interplay between non-conserved Lys residues and negatively charged conserved residues as well as the existence of a slightly different interaction network in the h5HT_{2B}R with respect to other class A GPCRs. However, it is still to be determined whether these differences can be ascribed to the biased signaling of the co-crystallized ligand, and hopefully future X-ray structures in complex with biased agonists will clarify this point.

Discussion

Rigid nucleosides also appear to be a privileged scaffold at diverse sites, in addition to purine receptors. In our repurposing of nucleosides to obtain novel 5HT₂R ligands, we utilized a structure-based approach. Similar methods could be suitable for the repurposing of scaffolds to other GPCRs. The lead for our present study originated from a fortuitous hit in the off-target screening of known AR ligands, i.e. the 5HT₂R interaction of **10**, but it is conceivable to structurally modify a given scaffold to fit to a GPCR target of choice purely using computational methods and not be dependent on fortuitous empirical screening. By repurposing a nucleoside scaffold from one set of GPCRs, i.e. ARs, to interact selectively with 5HT₂Rs as guided by structural information, we can create novel ligands with physicochemical characteristics that are different from known 5HT₂R ligands. The rational design of new GPCR ligands aided by computational analysis of new X-ray structures is gaining momentum.¹⁹

Several compounds demonstrated moderate selectivity for the 5HT₂Rs. Small alkyl esters **25** and **26** were the most potent in this series at 5HT_{2B}R, with **25** being slightly selective in binding with respect to 5HT_{2C}R. Both compounds were modestly selective in comparison to ARs, at which they display only μ M affinity. The corresponding 6-*N,N*-dimethylamino analogue **29** was less potent but still 5HT₂R-selective. An amino-propylamide **32** was moderately selective for 5HT_{2C}R in comparison to ARs. Moderate binding selectivity for the 5HT_{2B}R in comparison to 5HT_{2C}R was achieved with compounds **14**, **20**, **23** and **41**. In functional assays, 5'-amide **23**, which also bound to the A₃AR, was 5HT_{2B}R-selective, while **14**, **25** and **26** were nonselective. Several compounds in addition to **23** were mixed ligands at ARs and 5HT₂Rs. For example, **14** was a mixed potent ligand at A₁AR (agonist) and 5HT₂Rs (antagonist). Compounds **16** and **21** were mixed potent ligands at A₁AR/A₃AR and A₁AR (agonists), respectively, and at 5HT_{2B}R (likely antagonists). Compound **24** was a mixed ligand at A₃AR and 5HT_{2B/C}Rs. Thus, we have identified (N)-methanocarba nucleosides that favored 5HT_{2B}R affinity (Figure S4, Supporting Information, and in some cases also 5HT_{2C}R). The 5'-methyl or ethyl ester modification lowered affinity at the A₁AR by roughly 4-fold and at A₃AR by 10- to 20-fold. The effects of amide chain extension at the 5' position were complex and resulted in only modest selectivity.

Thus, we can tune the mixture of AR and 5HT₂R activities by structural manipulation to provide novel compounds displaying mixed activities within the two families of receptors or favoring activity at either family. The SAR herein determined is consistent with a previous prediction that the (N)-methanocarba nucleosides bind at the h5HT₂R_s in an orientation different from the presumed binding mode at the ARs (*i.e.* with the pseudo-sugar portion projecting into the TM bundle). The specific preference for the *N*⁶-dicyclopropylmethyl group is consistent with a small pocket at the TM5/TM6 interface. The modeling analysis herein presented suggests that ligand-recognition at the h5HT₂R_s might occur with the scaffold lying almost parallel to the membrane plane. In this position, the 5' group points toward the EL2 and the extracellular tip of TM5, a region exhibiting structural diversity in the h5HT₂R_s, thus revealing the potential for further derivatization at this position. In particular, the selection of suitable anchoring points among non-conserved residues might achieve selectivity at the desired h5HT₂R subtype.

The design of selective ligands of the 5HT_{2B}R is warranted based on recent biological findings. Selective antagonists might be useful for treating the heart or pulmonary hypertension.^{14,40} Their experimental use in liver protection has been demonstrated; 5HT_{2B}R blockade reduces chronic fibrosis and enhances hepatic regeneration.¹⁴ A₃AR is highly expressed in the liver, and its agonists are also of interest for the treatment of liver disease.²⁰ Thus, a combined agent with both 5HT_{2B}R antagonist and A₃AR agonist activity might have a synergistic benefit in the liver. The application of 5HT_{2B}R antagonists for treating irritable bowel syndrome was also proposed.^{2,18} However, one recent study comparing selective 5HT₂R antagonists failed to confirm that activity.⁴¹ A variety of approaches have contributed to recent efforts to discover selective 5HT₂R agonists and antagonists from screening and computational analysis. For example, computational activity prediction and microfluidics-assisted synthesis enabled the discovery of new 5HT_{2B}R antagonists.⁴² Other novel antagonists were discovered as a result of broad screening programs.^{43,44} Activity at the 5HT_{2A}R, considered to be a mechanism of hallucinogenic activity of a subset of its agonists,⁴⁵ is consistently low or absent throughout this compound series.

In general, 5HT₂R modulation in the brain contributes to the activity of antidepressant drugs. Various antidepressant drugs raise levels of 5HT, which can activate the 5HT_{2B}R and downregulate the 5HT_{2C}R to contribute to the action of these drugs. Inhibition of the 5HT_{2C}R, which forms functional GPCR heterodimers with the melatonin MT₂R,⁴⁶ has both antidepressant and anxiolytic effects. However, 5HT_{2B}R activation has antinociceptive properties related to the association of this subtype with descending inhibitory pain pathways originating in the rostroventral medial medulla (RVM).^{47–49} The typically low penetration of nucleoside derivatives into the brain⁵⁰ would be of benefit when applying 5HT_{2B}R antagonists for peripheral conditions such as cardiac and hepatic fibrosis. This might be an advantage of the nucleoside 5HT_{2B}R antagonists over brain penetrant heterocycles. We have not determined if the 5HT₂R antagonist activity in this chemical series represents neutral antagonism or inverse agonism, which has a bearing on potential therapeutic applications because of receptor constitutive activity.⁵¹ It was also noted that AR agonists might facilitate passage of various solutes across the blood brain barrier,⁵² but if this activity is removed from the current analogues, then that would not be a factor.

In conclusion, we have transformed rigid carbocyclic nucleosides that are A₃AR-selective agonists into moderately potent 5HT_{2B}R and/or 5HT_{2C}R antagonists using a structure-based approach. Although many of the compounds are nonselective between these two receptor subtypes, there is a tendency toward greater affinity at the 5HT_{2B}R. We have analyzed the molecular recognition in this chemical series, aided by the X-ray structural determination of rhodopsin-like GPCRs and the availability of broad screening, to shift and optimize the binding of the same scaffold to a new family of receptors.

Experimental section

Chemical synthesis

Materials and instrumentation—All reagents and solvents were purchased from Sigma-Aldrich (St. Louis, MO). ¹H NMR spectra were obtained with a Bruker 400 spectrometer using CDCl₃, CD₃OD and DMSO as solvents. Chemical shifts are expressed in δ values (ppm) with tetramethylsilane (δ 0.00) for CDCl₃ and water (δ 3.30) for CD₃OD. NMR spectra were collected with a Bruker AV spectrometer equipped with a z-gradient [¹H, ¹³C, ¹⁵N]-cryoprobe. TLC analysis was carried out on glass sheets precoated with silica gel F254 (0.2 mm) from Aldrich. The purity of final nucleoside derivatives was checked using a Hewlett–Packard 1100 HPLC equipped with a Zorbax SB-Aq 5 μm analytical column (50 × 4.6 mm; Agilent Technologies Inc., Palo Alto, CA). Mobile phase: linear gradient solvent system, 5 mM TBAP (tetrabutylammoniumdihydrogenphosphate)–CH₃CN from 80:20 to 0:100 in 13 min; the flow rate was 0.5 mL/min. Peaks were detected by UV absorption with a diode array detector at 230, 254, and 280 nm. All derivatives tested for biological activity showed >95% purity by HPLC analysis (detection at 254 nm). Low-resolution mass spectrometry was performed with a JEOL SX102 spectrometer with 6-kV Xe atoms following desorption from a glycerol matrix or on an Agilent LC/MS 1100 MSD, with a Waters (Milford, MA) Atlantis C18 column. High resolution mass spectroscopic (HRMS) measurements were performed on a proteomics optimized Q-TOF-2 (Micromass-Waters) using external calibration with polyalanine, unless noted. Observed mass accuracies are those expected based on known performance of the instrument as well as trends in masses of standard compounds observed at intervals during the series of measurements. Reported masses are observed masses uncorrected for this time-dependent drift in mass accuracy. All of the monosubstituted alkyne and branched amine intermediates were purchased from Sigma-Aldrich (St. Louis, MO), Small Molecules, Inc. (Hoboken, NJ), Anichem (North Brunswick, NJ), PharmaBlock, Inc. (Sunnyvale, CA), Frontier Scientific (Logan, UT) and Tractus (Perrineville, NJ).

(1R,2R,3S,4R,5S)-4-(2-Chloro-6-((dicyclopropylmethyl)amino)-9H-purin-9-yl)-1-(hydroxymethyl)bicyclo[3.1.0]hexane-2,3-diol (14): Dowex50 (27 mg) was added to a solution of compound **64** (49 mg, 0.11 mmol) in MeOH (2 mL) and water (1 mL) and the mixture stirred for 5 h at room temperature. After completion of reaction, the reaction mixture filtered and filtrate was evaporated under vacuum. The crude mixture was purified on flash silica gel column chromatography (CH₂Cl₂:MeOH = 30:1) to give compound **14** (37 mg, 84%) as a colorless foamy powder. ¹H NMR (CD₃OD, 400 MHz) δ 8.44 (s, 1H), 4.80 (s, 1H), 4.78 (d, *J* = 6.4 Hz, 1H), 4.29 (d, *J* = 11.6 Hz, 1H), 3.88 (d, *J* = 6.4 Hz, 1H),

3.49 (br s, 1H), 1.64-1.61 (m, 1H), 1.55-1.53 (m, 1H), 1.18-1.09 (m, 2H), 0.78-0.74 (m, 1H), 0.60-0.55 (m, 2H), 0.47-0.39 (m, 6H). HRMS calculated for C₁₉H₂₅ClN₅O₃ (M + H)⁺: 406.1646; found 406.1653.

(1R,2R,3S,4R,5S)-4-(2-Chloro-6-(pentan-3-ylamino)-9H-purin-9-yl)-1-

(hydroxymethyl)bicyclo[3.1.0]hexane-2,3-diol (15): Compound **15** (85%) was prepared from compound **65** following the method for compound **14**. ¹H NMR (CD₃OD, 400 MHz) δ 8.44 (s, 1H), 4.81 (s, 1H), 4.79 (d, *J* = 6.8 Hz, 1H), 4.29 (d, *J* = 11.6 Hz, 1H), 4.19 (br s, 1H), 3.89 (d, *J* = 6.8 Hz, 1H), 1.75-1.67 (m, 2H), 1.64-1.53 (m, 4H), 0.97 (t, *J* = 7.2 Hz, 6H), 0.78-0.75 (m, 1H). HRMS calculated for C₁₇H₂₅ClN₅O₃ (M + H)⁺: 382.1646; found 382.1647.

(1R,2R,3S,4R,5S)-4-(2-Chloro-6-(((1R)-cyclopropylpropyl)amino)-9H-purin-9-yl)-1-

(hydroxymethyl)bicyclo[3.1.0]hexane-2,3-diol (16): Compound **16** (73%) was prepared from compound **66** following the method for compound **14**. ¹H NMR (CD₃OD, 400 MHz) δ 8.44 (s, 1H), 4.80 (s, 1H), 4.79 (d, *J* = 6.4 Hz, 1H), 4.29 (d, *J* = 11.6 Hz, 1H), 3.88 (d, *J* = 6.4 Hz, 1H), 3.66 (br s, 1H), 1.88-1.72 (m, 2H), 1.64-1.61 (m, 1H), 1.55 (t, *J* = 5.2 Hz, 1H), 1.02-0.99 (m, 4H), 0.78-0.74 (m, 1H), 0.61-0.56 (m, 1H), 0.47-0.41 (m, 2H), 0.36-0.33 (m, 1H). HRMS calculated for C₁₈H₂₅ClN₅O₃ (M + H)⁺: 394.1646; found 394.1647.

(1R,2R,3S,4R,5S)-4-(2-Chloro-6-(((1R)-cyclopropylpropyl)amino)-9H-purin-9-yl)-1-

(hydroxymethyl)bicyclo[3.1.0]hexane-2,3-diol (17): Compound **17** (72%) was prepared from compound **67** following the method for compound **14**. ¹H NMR (CD₃OD, 400 MHz) δ 8.44 (s, 1H), 4.80 (s, 1H), 4.79 (d, *J* = 6.4 Hz, 1H), 4.29 (d, *J* = 11.6 Hz, 1H), 3.88 (d, *J* = 6.4 Hz, 1H), 3.67 (br s, 1H), 1.88-1.70 (m, 2H), 1.63-1.61 (m, 1H), 1.56 (t, *J* = 5.2 Hz, 1H), 1.02-0.99 (m, 4H), 0.78-0.75 (m, 1H), 0.59-0.56 (m, 1H), 0.45-0.42 (m, 2H), 0.36-0.30 (m, 1H). HRMS calculated for C₁₈H₂₅ClN₅O₃ (M + H)⁺: 394.1646; found 394.1642.

(1R,2R,3S,4R,5S)-4-(2-Chloro-6-(((1R)-cyclopropyl-2-methylpropyl)amino)-9H-

purin-9-yl)-1-(hydroxymethyl)bicyclo[3.1.0]hexane-2,3-diol (18): Compound **18** (67%) was prepared from compound **68** following the method for compound **14**. ¹H NMR (CD₃OD, 400 MHz) δ 8.44 (s, 1H), 4.80 (s, 1H), 4.79 (d, *J* = 6.4 Hz, 1H), 4.29 (d, *J* = 11.6 Hz, 1H), 3.89 (d, *J* = 6.4 Hz, 1H), 3.61 (br s, 1H), 2.09-2.02 (m, 1H), 1.64-1.62 (m, 1H), 1.54 (t, *J* = 5.2 Hz, 1H), 1.08-1.04 (m, 7H), 0.78-0.74 (m, 1H), 0.67-0.61 (m, 1H), 0.45-0.36 (m, 3H). HRMS calculated for C₁₉H₂₇ClN₅O₃ (M + H)⁺: 408.1802; found 408.1806.

(1R,2R,3S,4R,5S)-4-(2-Chloro-6-(((1S)-cyclopropyl-2-methylpropyl)amino)-9H-

purin-9-yl)-1-(hydroxymethyl)bicyclo[3.1.0]hexane-2,3-diol (19): Compound **19** (68%) was prepared from compound **69** following the method for compound **14**. ¹H NMR (CD₃OD, 400 MHz) δ 8.44 (s, 1H), 4.80 (s, 1H), 4.79 (d, *J* = 6.4 Hz, 1H), 4.29 (d, *J* = 11.6 Hz, 1H), 3.89 (d, *J* = 6.4 Hz, 1H), 3.61 (br s, 1H), 2.08-2.02 (m, 1H), 1.64-1.61 (m, 1H), 1.55 (t, *J* = 5.2 Hz, 1H), 1.08-1.04 (m, 7H), 0.78-0.74 (m, 1H), 0.66-0.61 (m, 1H), 0.45-0.36 (m, 3H). HRMS calculated for C₁₉H₂₇ClN₅O₃ (M + H)⁺: 408.1802; found 408.1798.

(1R,2R,3S,4R,5S)-4-(2-Chloro-6-(((S)-cyclobutyl(cyclopropyl)methyl)amino)-9H-

purin-9-yl)-1-(hydroxymethyl)bicyclo[3.1.0]hexane-2,3-diol (20): Compound **20** (69%)

was prepared from compound **70** following the method for compound **14**. ¹H NMR (CD₃OD, 400 MHz) δ 8.44 (s, 1H), 4.80 (s, 1H), 4.79 (d, *J* = 6.4 Hz, 1H), 4.29 (d, *J* = 11.6 Hz, 1H), 3.89-3.82 (m, 2H), 2.73-2.65 (m, 1H), 2.12-2.07 (m, 1H), 2.01-1.87 (m, 4H), 1.85-1.80 (m, 1H), 1.64-1.61 (m, 1H), 1.54 (t, *J* = 5.2 Hz, 1H), 0.97-0.91 (m, 1H), 0.78-0.74 (m, 1H), 0.58-0.53 (m, 1H), 0.40-0.36 (m, 3H). HRMS calculated for C₂₀H₂₇ClN₅O₃ (M + H)⁺: 420.1796; found 420.1796.

(1R,2R,3S,4R,5S)-4-(2-Chloro-6-(((R)-cyclobutyl(cyclopropyl)methyl)amino)-9H-purin-9-yl)-1-(hydroxymethyl)bicyclo[3.1.0]hexane-2,3-diol (21)

Compound **21** (69%) was prepared from compound **71** following the method for compound **14**. ¹H NMR (CD₃OD, 400 MHz) δ 8.44 (s, 1H), 4.80 (s, 1H), 4.79 (d, *J* = 6.4 Hz, 1H), 4.29 (d, *J* = 11.6 Hz, 1H), 3.89-3.82 (m, 2H), 2.71-2.67 (m, 1H), 2.12-2.07 (m, 1H), 2.01-1.87 (m, 4H), 1.83-1.80 (m, 1H), 1.64-1.61 (m, 1H), 1.54 (t, *J* = 5.2 Hz, 1H), 0.97-0.90 (m, 1H), 0.78-0.74 (m, 1H), 0.58-0.53 (m, 1H), 0.40-0.36 (m, 3H). HRMS calculated for C₂₀H₂₇ClN₅O₃ (M + H)⁺: 420.1802; found 420.1799.

(1R,2R,3S,4R,5S)-4-(2-Chloro-6-(dimethylamino)-9H-purin-9-yl)-1-(hydroxymethyl)bicyclo[3.1.0]hexane-2,3-diol (22)

10% TFA in water (1.5 mL) was added to a solution of compound **63** (16 mg, 0.02 mmol) in methanol (1.5 mL) and the mixture heated at 70 °C for 6 h. Solvent was evaporated under vacuum, and the residue was purified on flash silica gel silica chromatography (CH₂Cl₂:MeOH = 30:1) to give compound **22** (6 mg, 68%) as a syrup. ¹H NMR (CD₃OD, 400 MHz) δ 8.44 (s, 1H), 4.81 (s, 1H), 4.77 (d, *J* = 6.4 Hz, 1H), 4.30 (d, *J* = 11.6 Hz, 1H), 3.85 (d, *J* = 6.8 Hz, 1H), 3.49 (br s, 6H), 1.64-1.61 (m, 1H), 1.55 (d, *J* = 5.2 Hz, 1H), 0.78-0.75 (m, 1H). HRMS calculated for C₁₄H₂₃ClN₅O₃ (M + H)⁺: 340.1176; found 340.1177.

(1S,2R,3S,4R,5S)-4-(2-Chloro-6-((dicyclopropylmethyl)amino)-9H-purin-9-yl)-2,3-dihydroxy-N-methylbicyclo[3.1.0]hexane-1-carboxamide (23)

40% MeNH₂ solution (2 mL) was added to a solution of compound **26** (41 mg, 0.09 mmol) in MeOH (2 mL) and the mixture stirred overnight at room temperature. Solvent was evaporated, and the residue was purified on flash silica gel column chromatography (CH₂Cl₂:MeOH = 20:1) to give compound **23** (25 mg, 65%) as a syrup. ¹H NMR (CD₃OD, 400 MHz) δ 8.04 (s, 1H), 5.07 (d, *J* = 6.4 Hz, 1H), 4.80 (s, 1H), 4.01 (d, *J* = 6.4 Hz, 1H), 3.49 (br s, 1H), 2.87 (s, 3H), 2.08-2.04 (m, 1H), 1.82 (t, *J* = 4.8 Hz, 1H), 1.40-1.36 (m, 1H), 1.18-1.09 (m, 2H), 0.60-0.55 (m, 2H), 0.47-0.39 (m, 6H). HRMS calculated for C₂₀H₂₆ClN₆O₃ (M + H)⁺: 433.1755; found 433.1771.

(1S,2R,3S,4R,5S)-4-(2-Chloro-6-(dimethylamino)-9H-purin-9-yl)-2,3-dihydroxy-N-methylbicyclo[3.1.0]hexane-1-carboxamide (24)

Compound **24** (67%) was prepared from compound **29** following the method for compound **23**. ¹H NMR (CD₃OD, 400 MHz) δ 7.96 (s, 1H), 5.05 (d, *J* = 6.4 Hz, 1H), 4.80 (s, 1H), 3.99 (d, *J* = 6.4 Hz, 1H), 3.49 (br s, 6H), 2.87 (s, 3H), 2.06-2.04 (m, 1H), 1.83 (t, *J* = 4.8 Hz, 1H), 1.40-1.36 (m, 1H). HRMS calculated for C₁₅H₂₀ClN₆O₃ (M + H)⁺: 367.1285; found 367.1290.

Methyl (1S,2R,3S,4R,5S)-4-(2-Chloro-6-((dicyclopropylmethyl)amino)-9H-purin-9-yl)-2,3-dihydroxybicyclo[3.1.0]hexane-1-carboxylate (25): DCC (28 mg, 0.13 mmol) and DMAP (2.76 mg, 0.13 mmol) were added to a solution of compound **28** (19 mg, 0.04 mmol) in DMF (0.7 mL). After stirring the reaction mixture for 10 min at room temperature, anhydrous MeOH (6.0 μ L, 0.13 mmol) was added and the mixture stirred overnight at same condition. Solvent was evaporated, and the residue was purified on flash silica gel column chromatography (ethyl acetate:MeOH = 85:1) to give compound **25** (13 mg, 68%) as a syrup. $^1\text{H NMR}$ (CD_3OD , 400 MHz) δ 7.94 (s, 1H), 5.22 (d, J = 6.8 Hz, 1H), 4.78 (s, 1H), 4.07 (d, J = 6.4 Hz, 1H), 3.80 (s, 3H), 3.49 (br s, 1H), 2.19-2.15 (m, 1H), 1.88 (t, J = 4.8 Hz, 1H), 1.62-1.59 (m, 1H), 1.15-1.11 (m, 2H), 0.63-0.53 (m, 2H), 0.45-0.42 (m, 6H). HRMS calculated for $\text{C}_{20}\text{H}_{25}\text{ClN}_5\text{O}_4$ ($\text{M} + \text{H}$) $^+$: 434.1595; found 434.1603.

Ethyl (1S,2R,3S,4R,5S)-4-(2-chloro-6-((dicyclopropylmethyl)amino)-9H-purin-9-yl)-2,3-dihydroxybicyclo[3.1.0]hexane-1-carboxylate (26): Dowex50 (107 mg) was added to a solution of compound **76** (166 mg, 0.34 mmol) in MeOH (4 mL) and water (3 mL) and the mixture heated for 1 h at 65 $^\circ\text{C}$. After completion of reaction, the reaction mixture was filtered and the filtrate was evaporated under vacuum. The crude mixture was purified on flash silica gel column chromatography (hexane:ethyl acetate = 1:2) to give compound **26** (131 mg, 86%) as a colorless foamy powder. $^1\text{H NMR}$ (CD_3OD , 400 MHz) δ 7.96 (s, 1H), 5.23 (d, J = 6.8 Hz, 1H), 4.77 (s, 1H), 4.28-4.22 (m, 2H), 4.12 (d, J = 6.8 Hz, 1H), 3.49 (br s, 1H), 2.18-2.15 (m, 1H), 1.87 (t, J = 5.2 Hz, 1H), 1.63-1.60 (m, 1H), 1.32 (t, J = 7.2 Hz, 3H), 1.18-1.09 (m, 2H), 0.61-0.54 (m, 2H), 0.47-0.42 (m, 6H). HRMS calculated for $\text{C}_{21}\text{H}_{27}\text{ClN}_5\text{O}_4$ ($\text{M} + \text{H}$) $^+$: 448.1752; found 448.1745.

Propyl (1S,2R,3S,4R,5S)-4-(2-chloro-6-((dicyclopropylmethyl)amino)-9H-purin-9-yl)-2,3-dihydroxybicyclo[3.1.0]hexane-1-carboxylate (27): Compound **27** (66%) was prepared from compound **28** following the method for compound **25**. $^1\text{H NMR}$ (CD_3OD , 400 MHz) δ 7.95 (s, 1H), 5.23 (d, J = 6.4 Hz, 1H), 4.77 (s, 1H), 4.16 (t, J = 6.8 Hz, 2H), 4.10 (d, J = 6.4 Hz, 1H), 3.49 (br s, 1H), 2.19-2.16 (m, 1H), 1.88 (t, J = 4.8 Hz, 1H), 1.78-1.69 (m, 2H), 1.64-1.60 (m, 1H), 1.17-1.09 (m, 2H), 0.99 (t, J = 7.2 Hz, 3H), 0.61-0.54 (2H), 0.47-0.41 (m, 6H). HRMS calculated for $\text{C}_{22}\text{H}_{29}\text{ClN}_5\text{O}_4$ ($\text{M} + \text{H}$) $^+$: 462.1908; found 462.1903.

(1S,2R,3S,4R,5S)-4-(2-Chloro-6-((dicyclopropylmethyl)amino)-9H-purin-9-yl)-2,3-dihydroxybicyclo[3.1.0]hexane-1-carboxylic acid (28): 2N NaOH solution (1.5 mL) was added to a solution of compound **26** (39 mg, 0.08 mmol) in methanol (1.5 mL) and the mixture stirred at room temperature for 1.5 h. The reaction mixture was neutralized with acetic acid and evaporated under vacuum. The crude product was purified on flash silica gel column chromatography (CH_2Cl_2 :MeOH:TFA=20:1:0.1) to give compound **28** (27 mg, 76%) as colorless powder. $^1\text{H NMR}$ (CD_3OD , 400 MHz) δ 7.99 (s, 1H), 5.18 (d, J = 6.8 Hz, 1H), 4.79 (s, 1H), 4.10 (d, J = 6.8 Hz, 1H), 3.49 (br s, 1H), 2.19-2.16 (m, 1H), 1.90 (t, J = 5.2 Hz, 1H), 1.66-1.62 (m, 1H), 1.16-1.11 (m, 2H), 0.61-0.55 (m, 2H), 0.47-0.39 (m, 6H). HRMS calculated for $\text{C}_{19}\text{H}_{23}\text{ClN}_5\text{O}_4$ ($\text{M} + \text{H}$) $^+$: 420.1439; found 420.1438.

Ethyl (1S,2R,3S,4R,5S)-4-(2-chloro-6-(dimethylamino)-9H-purin-9-yl)-2,3-dihydroxybicyclo[3.1.0]hexane-1-carboxylate (29): 10% TFA in water (2.5 mL) was added to a solution of compound **77** (58 mg, 0.137 mmol) in methanol (2.5 mL) and the mixture heated at 70 °C for 3 h. Solvent was evaporated under vacuum, and the residue was purified on flash silica gel silica chromatography (CH₂Cl₂:MeOH = 40:1) to give compound **29** (46 mg, 88%) as a syrup. ¹H NMR (CD₃OD, 400 MHz) δ 7.88 (s, 1H), 5.22 (d, *J* = 6.4 Hz, 1H), 4.78 (s, 1H), 4.28-4.22 (m, 2H), 4.08 (d, *J* = 6.4 Hz, 1H), 3.49 (br s, 6H), 2.17-2.14 (m, 1H), 1.88 (t, *J* = 5.2 Hz, 1H), 1.64-1.60 (m, 1H), 1.32 (t, *J* = 7.2 Hz, 3H). HRMS calculated for C₁₆H₂₁ClN₅O₄ (M + H)⁺: 382.1282; found 382.1283.

(1S,2R,3S,4R,5S)-4-(2-Chloro-6-(dimethylamino)-9H-purin-9-yl)-2,3-dihydroxybicyclo[3.1.0]hexane-1-carboxylic acid (30): Compound **30** (77%) was prepared from compound **29** following the method for compound **28**. ¹H NMR (CD₃OD, 400 MHz) δ 7.89 (s, 1H), 5.16 (d, *J* = 6.4 Hz, 1H), 4.79 (s, 1H), 4.08 (d, *J* = 6.4 Hz, 1H), 3.63 (br s, 6H), 2.18-2.15 (m, 1H), 1.91 (t, *J* = 5.2 Hz, 1H), 1.66-1.62 (m, 1H). HRMS calculated for C₁₄H₁₇ClN₅O₄ (M + H)⁺: 354.0969; found 354.0969.

(1S,2R,3S,4R,5S)-N-(2-Aminoethyl)-4-(2-chloro-6-((dicyclopropylmethyl)amino)-9H-purin-9-yl)-2,3-dihydroxybicyclo[3.1.0]hexane-1-carboxamide (31): Ethylenediamine (1 mL) was added to a solution of compound **26** (19 mg, 0.04 mmol) in methanol (0.3 mL) and the mixture stirred for 3 days at room temperature. Solvent was evaporated, and the residue was purified on flash silica gel column chromatography (CH₂Cl₂:MeOH:NH₄OH = 9:1:0.1) to give compound **31** (12 mg, 63%) as a syrup. ¹H NMR (CD₃OD, 400 MHz) δ 8.07 (s, 1H), 5.13 (d, *J* = 6.4 Hz, 1H), 4.81 (s, 1H), 4.02 (d, *J* = 6.4 Hz, 1H), 3.45-3.39 (m, 2H), 2.84 (t, *J* = 6.4 Hz, 2H), 2.10-2.07 (m, 1H), 1.83 (t, *J* = 5.2 Hz, 1H), 1.42-1.38 (m, 1H), 1.18-1.09 (m, 2H), 0.60-0.55 (m, 2H), 0.46-0.39 (m, 6H). HRMS calculated for C₂₁H₂₉ClN₇O₃ (M + H)⁺: 462.2020; found 462.2021.

(1S,2R,3S,4R,5S)-N-(3-Aminopropyl)-4-(2-chloro-6-((dicyclopropylmethyl)amino)-9H-purin-9-yl)-2,3-dihydroxybicyclo[3.1.0]hexane-1-carboxamide (32): Compound **32** (64%) was prepared from compound **29** following the method for compound **31**. ¹H NMR (CD₃OD, 400 MHz) δ 8.04 (s, 1H), 5.13 (d, *J* = 6.4 Hz, 1H), 4.80 (s, 1H), 4.03 (d, *J* = 6.4 Hz, 1H), 3.47-3.38 (m, 2H), 2.82 (t, *J* = 7.2 Hz, 2H), 2.06-2.05 (m, 1H), 1.84-1.65 (m, 3H), 1.40-1.36 (m, 1H), 1.16-1.09 (m, 2H), 0.60-0.55 (m, 2H), 0.46-0.39 (m, 6H). HRMS calculated for C₂₂H₃₁ClN₇O₃ (M + H)⁺: 476.2177; found 476.2172.

(1S,2R,3S,4R,5S)-N-(2-Acetamidoethyl)-4-(2-chloro-6-((dicyclopropylmethyl)amino)-9H-purin-9-yl)-2,3-dihydroxybicyclo[3.1.0]hexane-1-carboxamide (33): Triethylamine (3.2 μL, 0.011 mmol) was added to a solution of compound **31** (3.61 mg, 0.007 mmol) and acetic acid *N*-hydroxysuccinimide ester (1.77 mg, 0.011 mmol) in DMF (1 mL) and the mixture stirred at room temperature overnight. Solvent was evaporated, and the residue was purified on flash silica gel column chromatography (CH₂Cl₂:MeOH=15:1) to give compound **33** (2.3 mg, 59%) as a syrup. ¹H NMR (CD₃OD, 400 MHz) δ 8.06 (s, 1H), 5.06 (d, *J* = 6.4 Hz, 1H), 4.81 (s, 1H), 4.01 (d, *J* = 6.4 Hz, 1H), 3.42-3.38 (m, 2H), 3.36-3.32 (m, 2H), 2.09-2.06 (m, 1H), 1.95 (s, 3H), 1.83 (t, *J* = 4.8 Hz,

1H), 1.40-1.37 (m, 1H), 1.17-1.09 (m, 2H), 0.60-0.56 (m, 2H), 0.55-0.44 (m, 6H). HRMS calculated for C₂₃H₃₁ClN₇O₄ (M + H)⁺: 504.2116; found 504.2126.

9-((3aR,3bR,4aS,5R,5aS)-3b-(((tert-Butyldiphenylsilyloxy)methyl)-2,2-dimethylhexahydrocyclopropa[3,4]cyclopenta[1,2-d][1,3]dioxol-5-yl)-2,3-dihydroxybicyclo[3.1.0]hexane-1-carboxamide (34): Compound **34** (58%) was prepared from compound **32** following the method for compound **33**. ¹H NMR (CD₃OD, 400 MHz) δ 8.09 (s, 1H), 5.06 (d, *J* = 6.4 Hz, 1H), 4.80 (s, 1H), 4.02 (d, *J* = 6.4 Hz, 1H), 3.51 (br s, 1H), 3.27-3.23 (m, 4H), 2.09-2.06 (m, 1H), 1.96 (s, 3H), 1.84 (t, *J* = 5.2 Hz, 1H), 1.76 (t, *J* = 6.8 Hz, 2H), 1.41-1.37 (m, 1H), 1.18-1.09 (m, 2H), 0.60-0.55 (m, 2H), 0.47-0.39 (m, 6H). HRMS calculated for C₂₄H₃₃ClN₇O₄ (M + H)⁺: 518.2283; found 518.2289.

9-((3aR,3bR,4aS,5R,5aS)-3b-(((tert-Butyldiphenylsilyloxy)methyl)-2,2-dimethylhexahydrocyclopropa[3,4]cyclopenta[1,2-d][1,3]dioxol-5-yl)-2,6-dichloro-9H-purine (54): DIAD (0.17 mL, 0.89 mmol) was added to a solution of 2,6-dichloropurine (170 mg, 0.89 mmol) and triphenylphosphine (235 mg, 0.89 mmol) in THF (4 mL) at 0 °C and the mixture was stirred for 20 min at room temperature. A solution of compound **53** (197 mg, 0.49 mmol) in THF (2 mL) was added into the reaction mixture and the mixture stirred overnight at room temperature. Solvent was evaporated, and the residue was purified on flash silica gel column chromatography (hexane:ethyl acetate=5:1) to give compound **54** (189 mg, 69%) as colorless foamy powder. ¹H NMR (CDCl₃, 400 MHz) δ 8.42 (s, 1H), 7.63-7.61 (m, 4H), 7.42-7.31 (m, 6H), 5.28 (d, *J* = 6.4 Hz, 1H), 5.09 (s, 1H), 4.58 (d, *J* = 7.2 Hz, 1H), 4.29 (d, *J* = 10.8 Hz, 1H), 3.70 (d, *J* = 10.8 Hz, 1H), 1.59-1.58 (m, 1H), 1.55 (s, 3H), 1.25 (s, 3H), 1.17-1.15 (s, 1H), 1.11 (s, 9H), 1.07-1.04 (m, 1H). HRMS calculated for C₃₁H₃₅Cl₂SiN₄O₃ (M + H)⁺: 609.1856; found 609.1857.

9-((3aR,3bR,4aS,5R,5aS)-3b-(((tert-Butyldiphenylsilyloxy)methyl)-2,2-dimethylhexahydrocyclopropa[3,4]cyclopenta[1,2-d][1,3]dioxol-5-yl)-2-chloro-N-(dicyclopropylmethyl)-9H-purin-6-amine (55): 2,2-Dicyclopropyl-methylamine (80 mg, 0.54 mmol) and triethylamine (0.25 mL, 1.8 mmol) were added to a solution of compound **54** (110, 0.18 mmol) in methanol (4 mL) and the mixture stirred at room temperature overnight. The reaction mixture was evaporated under vacuum, and the residue was purified on flash column chromatography (hexane:ethyl acetate = 4:1) to give the desired product **55** (105 mg, 85%) as a syrup. ¹H NMR (CDCl₃, 400 MHz) δ 8.06 (s, 1H), 7.66-7.62 (m, 4H), 7.44-7.33 (m, 6H), 5.29 (d, *J* = 6.4 Hz, 1H), 5.02 (s, 1H), 4.58 (d, *J* = 7.2 Hz, 1H), 4.30 (d, *J* = 10.8 Hz, 1H), 3.63-3.60 (m, 2H), 1.61-1.58 (m, 1H), 1.54 (s, 3H), 1.29-1.25 (m, 4H), 1.08 (s, 9H), 1.07-1.03 (m, 2H), 0.98-0.94 (m, 1H), 0.60-0.44 (m, 8H). HRMS calculated for C₃₈H₄₇ClSiN₅O₃ (M + H)⁺: 684.3131; found 684.3132.

9-((3aR,3bR,4aS,5R,5aS)-3b-(((tert-Butyldiphenylsilyloxy)methyl)-2,2-dimethylhexahydrocyclopropa[3,4]cyclopenta[1,2-d][1,3]dioxol-5-yl)-2-chloro-N-(pentan-3-yl)-9H-purin-6-amine (56): Compound **56** (81%) was prepared from compound **54** following the method for compound **55**. ¹H NMR (CD₃OD, 400 MHz) δ 8.26 (s, 1H), 7.66-7.64 (m, 4H), 7.43-7.31 (m, 6H), 5.35 (d, *J* = 6.8 Hz, 1H), 4.95 (s, 1H), 4.71 (d, *J* = 6.8 Hz, 1H), 4.23 (d, *J* = 10.4 Hz, 1H), 3.76 (d, *J* = 10.4 Hz, 1H), 1.76-1.69 (m, 2H), 1.63-1.56

(m, 3H), 1.52 (s, 3H), 1.26 (s, 3H), 1.14-1.11 (m, 1H), 1.09 (s, 9H), 1.02-0.95 (m, 8H).
HRMS calculated for C₃₆H₄₇ClSiN₅O₃ (M + H)⁺: 660.3137; found 660.3135.

9-((3aR,3bR,4aS,5R,5aS)-3b-(((tert-Butyldiphenylsilyloxy)methyl)-2,2-dimethylhexahydrocyclopropa[3,4]cyclopenta[1,2-d][1,3]dioxol-5-yl)-2-chloro-N-((1R)-cyclopropylpropyl)-9H-purin-6-amine (57): Compound **57** (83%) was prepared from compound **54** following the method for compound **55**. ¹H NMR (CD₃OD, 400 MHz) δ 8.25 (s, 1H), 7.65-7.63 (m, 4H), 7.44-7.33 (m, 6H), 5.34 (d, *J* = 7.0 Hz, 1H), 4.94 (s, 1H), 4.70 (d, *J* = 7.0 Hz, 1H), 4.22 (d, *J* = 10.4 Hz, 1H), 3.77 (d, *J* = 10.4 Hz, 1H), 3.69 (br s, 1H), 1.90-1.72 (m, 2H), 1.61-1.60 (m, 1H), 1.52 (s, 3H), 1.26 (s, 3H), 1.13-1.10 (m, 1H), 1.08 (s, 9H), 1.06-1.02 (m, 4H), 0.98-0.95 (m, 1H), 0.63-0.56 (m, 1H), 0.48-0.40 (m, 2H), 0.37-0.32 (m, 1H). HRMS calculated for C₃₇H₄₇ClSiN₅O₃ (M + H)⁺: 672.3137; found 672.3127.

9-((3aR,3bR,4aS,5R,5aS)-3b-(((tert-Butyldiphenylsilyloxy)methyl)-2,2-dimethylhexahydrocyclopropa[3,4]cyclopenta[1,2-d][1,3]dioxol-5-yl)-2-chloro-N-((1S)-cyclopropylpropyl)-9H-purin-6-amine (58): Compound **58** (82%) was prepared from compound **54** following the method for compound **55**. ¹H NMR (CD₃OD, 400 MHz) δ 8.25 (s, 1H), 7.66-7.64 (m, 4H), 7.43-7.33 (m, 6H), 5.34 (d, *J* = 7.0 Hz, 1H), 4.94 (s, 1H), 4.70 (d, *J* = 7.0 Hz, 1H), 4.22 (d, *J* = 10.4 Hz, 1H), 3.77 (d, *J* = 10.4 Hz, 1H), 3.68 (br s, 1H), 1.88-1.72 (m, 2H), 1.62-1.60 (m, 1H), 1.52 (s, 3H), 1.26 (s, 3H), 1.13-1.08 (m, 1H), 1.08 (s, 9H), 1.04-1.00 (m, 4H), 0.99-0.95 (m, 1H), 0.62-0.57 (m, 1H), 0.48-0.44 (m, 2H), 0.38-0.35 (m, 1H). HRMS calculated for C₃₇H₄₇ClSiN₅O₃ (M + H)⁺: 672.3137; found 672.3136.

9-((3aR,3bR,4aS,5R,5aS)-3b-(((tert-Butyldiphenylsilyloxy)methyl)-2,2-dimethylhexahydrocyclopropa[3,4]cyclopenta[1,2-d][1,3]dioxol-5-yl)-2-chloro-N-((1R)-cyclopropyl-2-methylpropyl)-9H-purin-6-amine (59): Compound **59** (81%) was prepared from compound **54** following the method for compound **55**. ¹H NMR (CD₃OD, 400 MHz) δ 8.26 (s, 1H), 7.66-7.64 (m, 4H), 7.42-7.31 (m, 6H), 5.33 (d, *J* = 6.8 Hz, 1H), 4.94 (s, 1H), 4.71 (d, *J* = 6.8 Hz, 1H), 4.23 (d, *J* = 10.8 Hz, 1H), 3.75 (d, *J* = 10.8 Hz, 1H), 3.64 (t, *J* = 6.4 Hz, 1H), 2.09-2.02 (m, 1H), 1.62-1.59 (m, 1H), 1.52 (s, 3H), 1.26 (s, 3H), 1.16-1.02 (m, 16H), 1.01-0.90 (m, 2H), 0.66-0.61 (m, 1H), 0.46-0.37 (m, 3H). HRMS calculated for C₃₈H₄₉ClSiN₅O₃ (M + H)⁺: 686.3293; found 686.3293.

9-((3aR,3bR,4aS,5R,5aS)-3b-(((tert-Butyldiphenylsilyloxy)methyl)-2,2-dimethylhexahydrocyclopropa[3,4]cyclopenta[1,2-d][1,3]dioxol-5-yl)-2-chloro-N-((1S)-cyclopropyl-2-methylpropyl)-9H-purin-6-amine (60): Compound **60** (81%) was prepared from compound **54** following the method for compound **56**. ¹H NMR (CD₃OD, 400 MHz) δ 8.27 (s, 1H), 7.66-7.64 (m, 4H), 7.43-7.32 (m, 6H), 5.34 (d, *J* = 6.8 Hz, 1H), 4.95 (s, 1H), 4.71 (d, *J* = 6.8 Hz, 1H), 4.23 (d, *J* = 10.8 Hz, 1H), 3.74 (d, *J* = 10.8 Hz, 1H), 3.64 (t, *J* = 6.4 Hz, 1H), 2.11-2.02 (m, 1H), 1.63-1.60 (m, 1H), 1.52 (s, 3H), 1.26 (s, 3H), 1.15-1.05 (m, 16H), 0.99-0.93 (m, 2H), 0.67-0.63 (m, 1H), 0.46-0.40 (m, 3H). HRMS calculated for C₃₈H₄₉ClSiN₅O₃ (M + H)⁺: 686.3293; found 686.3298.

9-((3aR,3bR,4aS,5R,5aS)-3b-(((tert-Butyldiphenylsilyloxy)methyl)-2,2-dimethylhexahydrocyclopropa[3,4]cyclopenta[1,2-d][1,3]dioxol-5-yl)-2-chloro-N-((S)-

cyclobutyl(cyclopropyl)methyl-9H-purin-6-amine (61): Compound **61** (78%) was prepared from compound **54** following the method for compound **55**. ¹H NMR (CD₃OD, 400 MHz) δ 8.25 (s, 1H), 7.66- 7.64 (m, 4H), 7.43-7.31 (m, 6H), 5.33 (d, *J* = 6.8 Hz, 1H), 4.94 (s, 1H), 4.71 (d, *J* = 6.8 Hz, 1H), 4.23 (d, *J* = 10.4 Hz, 1H), 3.87 (br s, 1H), 3.77 (d, *J* = 10.4 Hz, 1H), 2.73-2.69 (m, 1H), 2.17-2.08 (m, 1H), 2.01-1.84 (m, 5H), 1.61-1.60 (m, 1H), 1.52 (s, 3H), 1.26 (s, 3H), 1.14-1.07 (m, 10H), 0.99-0.93 (m, 2H), 0.59-0.56 (m, 1H), 0.38-0.37 (m, 3H). HRMS calculated for C₃₉H₄₉ClSiN₅O₃ (M + H)⁺: 698.3293; found 698.3303.

9-((3aR,3bR,4aS,5R,5aS)-3b-(((tert-Butyldiphenylsilyloxy)methyl)-2,2-dimethylhexahydrocyclopropa[3,4]cyclopenta[1,2-d][1,3]dioxol-5-yl)-2-chloro-N-((R)-cyclobutyl(cyclopropyl)methyl)-9H-purin-6-amine (62): Compound **62** (79%) was prepared from compound **54** following the method for compound **55**. ¹H NMR (CD₃OD, 400 MHz) δ 8.25 (s, 1H), 7.66- 7.64 (m, 4H), 7.45-7.31 (m, 6H), 5.34 (d, *J* = 6.8 Hz, 1H), 4.94 (s, 1H), 4.71 (d, *J* = 6.8 Hz, 1H), 4.23 (d, *J* = 10.4 Hz, 1H), 3.86 (br s, 1H), 3.77 (d, *J* = 10.4 Hz, 1H), 2.72-2.68 (m, 1H), 2.12-2.08 (m, 1H), 1.99-1.84 (m, 5H), 1.62-1.61 (m, 1H), 1.52 (s, 3H), 1.26 (s, 3H), 1.16-1.04 (m, 10H), 0.99-0.93 (m, 2H), 0.57-0.55 (m, 1H), 0.39-0.37 (m, 3H). HRMS calculated for C₃₉H₄₉ClSiN₅O₃ (M + H)⁺: 698.3293; found 698.3281.

9-((3aR,3bR,4aS,5R,5aS)-3b-(((tert-Butyldiphenylsilyloxy)methyl)-2,2-dimethylhexahydrocyclopropa[3,4]cyclopenta[1,2-d][1,3]dioxol-5-yl)-2-chloro-N,N-dimethyl-9H-purin-6-amine (63): Compound **63** (84%) was prepared from compound **54** following the method for compound **55**. ¹H NMR (CD₃OD, 400 MHz) δ 8.11 (s, 1H), 7.66-7.62 (m, 4H), 7.41-7.30 (m, 6H), 5.32 (d, *J* = 6.8 Hz, 1H), 4.91 (s, 1H), 4.72 (d, *J* = 6.8 Hz, 1H), 4.17 (d, *J* = 10.8 Hz, 1H), 3.86 (d, *J* = 10.8 Hz, 1H), 3.49 (br s, 6H), 1.58-1.52 (m, 4H), 1.26 (s, 3H), 1.11-1.06 (m, 10H), 0.99-0.95 (m, 1H). HRMS calculated for C₃₃H₄₁ClSiN₅O₃ (M + H)⁺: 618.2667; found 618.2675.

(((3aR,3bR,4aS,5R,5aS)-5-(2-Chloro-6-(pentan-3-ylamino)-9H-purin-9-yl)-2,2-dimethyltetrahydrocyclopropa[3,4]cyclopenta[1,2-d][1,3]dioxol-3b(3aH)-yl)methanol (65): TBAF (0.08 mL, 1 M solution in THF) was added to a solution of compound **56** (39 mg, 0.06 mmol) in THF (2 mL) and the mixture stirred for 1 h at room temperature. Solvent was evaporated under vacuum, and the residue was purified on flash silica gel column chromatography (hexane:ethyl acetate = 1:1) to give compound **65** (16.8 mg, 68%) as a colorless syrup. ¹H NMR (CD₃OD, 400 MHz) δ 8.21 (s, 1H), 5.37 (d, *J* = 6.4 Hz, 1H), 4.95 (s, 1H), 4.70 (d, *J* = 6.8 Hz, 1H), 4.21-4.19 (m, 1H), 4.01 (d, *J* = 11.6 Hz, 1H), 3.62 (d, *J* = 11.6 Hz, 1H), 1.75-1.68 (m, 3H), 1.62-1.55 (m, 2H), 1.52 (s, 3H), 1.26 (s, 3H), 1.15 (t, *J* = 5.2 Hz, 1H), 1.00-0.93 (m, 7H). HRMS calculated for C₂₀H₂₉ClN₅O₃ (M + H)⁺: 422.1959; found 422.1954.

(((3aR,3bR,4aS,5R,5aS)-5-(2-Chloro-6-(((1R)-cyclopropylpropyl)amino)-9H-purin-9-yl)-2,2-dimethyltetrahydrocyclopropa[3,4]cyclopenta[1,2-d][1,3]dioxol-3b(3aH)-yl)methanol (66): Compound **66** (78%) was prepared from compound **57** following the method for compound **65**. ¹H NMR (CD₃OD, 400 MHz) δ 8.21 (s, 1H), 5.39 (d, *J* = 6.8 Hz,

1H), 4.95 (s, 1H), 4.70 (d, $J = 6.4$ Hz, 1H), 4.00 (d, $J = 11.6$ Hz, 1H), 3.67-3.65 (br m, 1H), 3.62 (d, $J = 11.6$ Hz, 1H), 1.88-1.81 (m, 1H), 1.77-1.68 (m, 2H), 1.52 (s, 3H), 1.26 (s, 3H), 1.15 (t, $J = 5.2$ Hz, 1H), 1.04-0.97 (m, 5H), 0.61-0.56 (m, 1H), 0.47-0.40 (m, 2H), 0.36-0.33 (m, 1H). HRMS calculated for $C_{21}H_{29}ClN_5O_3$ (M + H)⁺: 434.1959; found 434.1962.

((3aR,3bR,4aS,5R,5aS)-5-(2-Chloro-6-(((1S)-cyclopropylpropyl)amino)-9H-purin-9-yl)-2,2-dimethyltetrahydrocyclopropa[3,4]cyclopenta[1,2-d][1,3]dioxol-3b(3aH)-yl)methanol (67): Compound **67** (79%) was prepared from compound **58** following the method for compound **65**. ¹H NMR (CD₃OD, 400 MHz) δ 8.21 (s, 1H), 5.39 (d, $J = 6.8$ Hz, 1H), 4.95 (s, 1H), 4.70 (d, $J = 6.4$ Hz, 1H), 4.01 (d, $J = 11.6$ Hz, 1H), 3.67-3.65 (br m, 1H), 3.62 (d, $J = 11.6$ Hz, 1H), 1.88-1.81 (m, 1H), 1.75-1.68 (m, 2H), 1.52 (s, 3H), 1.26 (s, 3H), 1.14 (t, $J = 5.2$ Hz, 1H), 1.03-0.95 (m, 5H), 0.62-0.55 (m, 1H), 0.44-0.41 (m, 2H), 0.36-0.33 (m, 1H). HRMS calculated for $C_{21}H_{29}ClN_5O_3$ (M + H)⁺: 434.1959; found 434.1952.

((3aR,3bR,4aS,5R,5aS)-5-(2-Chloro-6-(((1R)-cyclopropyl-2-methylpropyl)amino)-9H-purin-9-yl)-2,2-dimethyltetrahydrocyclopropa[3,4]cyclopenta[1,2-d][1,3]dioxol-3b(3aH)-yl)methanol (68): Compound **68** (80%) was prepared from compound **59** following the method for compound **65**. ¹H NMR (CD₃OD, 400 MHz) δ 8.21 (s, 1H), 5.39 (d, $J = 6.4$ Hz, 1H), 4.95 (s, 1H), 4.70 (d, $J = 6.8$ Hz, 1H), 4.00 (d, $J = 11.6$ Hz, 1H), 3.62-3.59 (m, 2H), 2.08-2.02 (m, 1H), 1.72-1.68 (m, 1H), 1.52 (s, 3H), 1.26 (s, 3H), 1.15 (t, $J = 5.2$ Hz, 1H), 1.08-1.03 (m, 7H), 0.99-0.97 (m, 1H), 0.65-0.62 (m, 1H), 0.43-0.36 (m, 3H). HRMS calculated for $C_{22}H_{31}ClN_5O_3$ (M + H)⁺: 448.2115; found 448.2112.

((3aR,3bR,4aS,5R,5aS)-5-(2-Chloro-6-(((1S)-cyclopropyl-2-methylpropyl)amino)-9H-purin-9-yl)-2,2-dimethyltetrahydrocyclopropa[3,4]cyclopenta[1,2-d][1,3]dioxol-3b(3aH)-yl)methanol (69): Compound **69** (79%) was prepared from compound **60** following the method for compound **65**. ¹H NMR (CD₃OD, 400 MHz) δ 8.21 (s, 1H), 5.38 (d, $J = 6.4$ Hz, 1H), 4.95 (s, 1H), 4.70 (d, $J = 6.8$ Hz, 1H), 4.00 (d, $J = 11.6$ Hz, 1H), 3.62-3.59 (m, 2H), 2.08-2.03 (m, 1H), 1.72-1.68 (m, 1H), 1.52 (s, 3H), 1.26 (s, 3H), 1.14 (t, $J = 5.2$ Hz, 1H), 1.08-1.04 (m, 7H), 0.99-0.95 (m, 1H), 0.66-0.61 (m, 1H), 0.42-0.36 (m, 3H). HRMS calculated for $C_{22}H_{31}ClN_5O_3$ (M + H)⁺: 448.2115; found 448.2115.

((3aR,3bR,4aS,5R,5aS)-5-(2-Chloro-6-(((S)-cyclobutyl(cyclopropyl)methyl)amino)-9H-purin-9-yl)-2,2-dimethyltetrahydrocyclopropa[3,4]cyclopenta[1,2-d][1,3]dioxol-3b(3aH)-yl)methanol (70): Compound **70** (77%) was prepared from compound **61** following the method for compound **65**. ¹H NMR (CD₃OD, 400 MHz) δ 8.21 (s, 1H), 5.39 (d, $J = 6.4$ Hz, 1H), 4.95 (s, 1H), 4.68 (d, $J = 6.4$ Hz, 1H), 4.01 (d, $J = 11.6$ Hz, 1H), 3.86-3.82 (m, 1H), 3.62 (d, $J = 11.6$ Hz, 1H), 2.71-2.63 (m, 1H), 2.12-2.09 (m, 1H), 2.02-1.86 (m, 3H), 1.83-1.80 (m, 1H), 1.73-1.68 (m, 1H), 1.52 (s, 3H), 1.26 (s, 3H), 1.15 (t, $J = 5.2$ Hz, 1H), 0.99-0.86 (m, 3H), 0.58-0.53 (m, 1H), 0.40-0.36 (m, 3H). HRMS calculated for $C_{23}H_{31}ClN_5O_3$ (M + H)⁺: 460.2115; found 460.2109.

((3aR,3bR,4aS,5R,5aS)-5-(2-Chloro-6-(((R)-cyclobutyl(cyclopropyl)methyl)amino)-9H-purin-9-yl)-2,2-dimethyltetrahydrocyclopropa[3,4]cyclopenta[1,2-d][1,3]dioxol-3b(3aH)-yl)methanol (71): Compound **71** (78%) was prepared from compound

62 following the method for compound **65**. ¹H NMR (CD₃OD, 400 MHz) δ 8.21 (s, 1H), 5.39 (d, *J* = 6.4 Hz, 1H), 4.95 (s, 1H), 4.70 (d, *J* = 6.4 Hz, 1H), 4.01 (d, *J* = 11.6 Hz, 1H), 3.87-3.84 (m, 1H), 3.62 (d, *J* = 11.6, Hz, 1H), 2.71-2.67 (m, 1H), 2.12-2.09 (m, 1H), 2.02-1.87(m, 3H), 1.83-1.80 (m, 1H), 1.71-1.68 (m, 1H), 1.52 (s, 3H), 1.26 (s, 3H), 1.15 (t, *J* = 5.2 Hz, 1H), 0.99-0.86 (m, 3H), 0.58-0.53 (m, 1H), 0.40-0.36 (m, 3H). HRMS calculated for C₂₃H₃₁ClN₅O₃ (M + H)⁺: 460.2115; found 460.2107.

Ethyl (3*aR*,3*bS*,4*aS*,5*R*,5*aS*)-5-(2-chloro-6-((dicyclopropylmethyl)amino)-9*H*-purin-9-yl)-2,2-dimethyltetrahydrocyclopropa[3,4]cyclopenta[1,2-*d*][1,3]dioxole-3*b*(3*aH*)-carboxylate (76): 2,2-Dicyclopropyl-methylamine (244 mg, 1.94 mmol) and triethylamine (0.53 mL, 3.9 mmol) were added to a solution of compound **75** (161, 0.39 mmol) in methanol (5 mL) and the mixture stirred at room temperature overnight. The reaction mixture was evaporated under vacuum, and the residue was purified on flash column chromatography (hexane:ethyl acetate = 3:1) to give the desired product **76** (166 mg, 87%) as a syrup. ¹H NMR (CD₃OD, 400 MHz) δ 8.03 (s, 1H), 5.86 (d, *J* = 6.8 Hz, 1H), 4.96 (s, 1H), 4.80 (d, *J* = 6.8 Hz, 1H), 4.28-4.18 (m, 2H), 3.45 (br s, 1H), 2.27-2.23 (m, 1H), 1.68-1.64 (m, 1H), 1.54-1.51 (m, 4H), 1.33 (t, *J* = 7.2 Hz, 3H), 1.34 (s, 3H), 1.17-1.10 (m, 2H), 0.60-0.54 (m, 2H), 0.46-0.38 (m, 6H). HRMS calculated for C₂₄H₃₁ClN₅O₄ (M + H)⁺: 488.2065; found 488.2065.

Ethyl (3*aR*,3*bS*,4*aS*,5*R*,5*aS*)-5-(2-chloro-6-(dimethylamino)-9*H*-purin-9-yl)-2,2-dimethyltetrahydrocyclopropa[3,4]cyclopenta[1,2-*d*][1,3]dioxole-3*b*(3*aH*)-carboxylate (77): Compound **77** (85%) was prepared from compound **75** following the method for compound **76**. ¹H NMR (CD₃OD, 400 MHz) δ 7.95 (s, 1H), 5.87 (d, *J* = 6.4 Hz, 1H), 4.94 (s, 1H), 4.83 (d, *J* = 6.4 Hz, 1H), 4.28-4.19 (m, 2H), 3.49 (br s, 6H), 2.25-2.21 (m, 1H), 1.67-1.63 (m, 1H), 1.53-1.55 (m, 4H), 1.34 (t, *J* = 7.2 Hz, 3H), 1.29 (s, 3H). HRMS calculated for C₁₉H₂₅ClN₅O₄ (M + H)⁺: 422.1595; found 422.1591.

Binding to ARs, 5HT₂R_s and to other diverse sites

Binding assays at ARs was performed as described.^{15,25} K_i determinations using 96-well plates and binding profiles in a broad screen of receptors and channels were generously provided by the National Institute of Mental Health's Psychoactive Drug Screening Program, Contract # HHSN-271-2008-00025-C (NIMH PDSP). The NIMH PDSP is Directed by Bryan L. Roth MD, PhD at the University of North Carolina at Chapel Hill and Project Officer Jamie Driscoll at NIMH, Bethesda MD, USA. For experimental details please refer to the PDSP web site <http://pdsp.med.unc.edu/> and click on "Binding Assay" or "Functional Assay" on the menu bar. The cell line used for preparing membranes for h5HT_{2A}R binding is transiently transfected HEKT cells, grown in DMEM medium containing 10% serum. Stable HEK cells were used for preparing membranes for h5HT_{2B}R binding and grown in medium containing 2 µg/mL Puromycin. Flp-In HEK cells were used for preparing membranes for h5HT_{2C}R binding and grown in DMEM medium containing 100 µg/mL Hygromycin B. Radioligands used and their measured 5HT₂R affinities from saturation experiments are given in Table 1. The binding buffer consisted of 50 mM Tris.HCl, 10 mM MgCl₂, 0.1 mM EDTA at pH 7.4 and at RT, and the wash buffer was cold 50 mM Tris.HCl at pH 7.4. Nonspecific binding was determined as noted in Table 1. Untransfected HEK-293

cells do not express specific [³H]43 binding.⁵⁴ Where we use a nonspecific radioligand, [³H]43, and an antagonist of broad specificity (10 μM clozapine for 5HT_{2A}) to define nonspecific binding, only the receptor of interest is detected as specific binding because it is overexpressed in HEK cells. Although only a single 5HT receptor was overexpressed in the HEK cells, it is possible that [³H]43 binds to endogenous serotonin or non-serotonin receptors with affinities within the nanomolar range in these cells. Results were analyzed in Prism 5.0 by nonlinear least-squares regression to obtain K_i values. Statistical significance of the difference was assessed using unpaired t-test or One-Way Analysis of Variance (ANOVA) followed by post-hoc test where appropriate.

Functional assays at 5HT₂Rs

In functional assays, the 5HT_{2A}R, 5HT_{2B}R and 5HT_{2C}R were expressed in Flp-In HEK cells. Cells were plated into poly-L-lysine coated 96-well black clear bottom cell culture plates with DMEM supplemented with 1% dialyzed FBS and cultured overnight before assays. Activity an agonist or antagonist (using 5-HT as reference agonist at the EC₈₀) was determined in calcium mobilization experiments using a FLIPR^{TETRA} (Molecular Devices, Sunnyvale, CA). Plates were loaded with the Fluo-4 Direct Calcium dye (prepared in 20 mM HEPES, 1× HBSS, 2.5 mM Probenecid, pH 7.4) and incubated for 60 min at 37°C, followed by a 10 min incubation at room temperature in the dark. The FLIPR then collected 10 readings (1 read per second) first as a baseline before addition of solutions of the test compound. For agonist activity, the fluorescence intensity was recorded for 2 min after test compound addition. To measure antagonist activity, test compound stocks were prepared at 4× of the final concentration and added as above for potential effects on basal levels for 2 min first, followed by a 5 to 10 min incubation before addition of reference agonist 5-HT at a final concentration equivalent to the EC₈₀ to measure remaining agonist activity.

Maximal fluorescence intensity (RFU) was recorded within a min after drug addition. IC₅₀ values obtained were converted to K_i values using the Cheng-Prusoff equation.⁵³ The FLIPR calcium assay does not differentiate between inverse agonist and neutral antagonist activity. In control HEK293 cells, there was no endogenous response to 5-HT, using either calcium transients in functional assays or specific radioligand binding assays (results not shown). Comparison between experimental curves was performed using F-test ($P < 0.05$ was considered as statistically significant).

Preclinical testing

Parameters in Table 2 were determined by GVK BIO Sciences Pvt Ltd Hyderabad, India.

Molecular Modeling

Computational facilities—Ligand geometry optimization, homology modeling and molecular docking simulations were carried out using a 6 Intel® Xeon® E5-1650 v3 CPU workstation. Membrane MD simulations were run in part on an in-house cluster composed of two NVIDIA® 970 GTX and one NVIDIA® 980Ti GTX, and in part by exploiting the computational resources (four NVIDIA® Tesla® K20X) of the NIH HPC Biowulf cluster (<http://biowulf.nih.gov>).

Ligand Preparation—Selected compounds were built using Maestro⁵⁵ and subjected to gas phase geometry optimization with the Jaguar 8.9 quantum chemistry package⁵⁶ using density functional theory (DFT) with the B3LYP hybrid functional and the 6-31G** basis set. Frequency calculations were performed to ensure the structures represented minima on the potential energy surfaces.

Homology modeling—The h5HT_{2B}R homology model was built upon the X-ray structure of the ERG-h5HT_{2B}R complex.¹¹ The template structure was retrieved from the RCSB PDB database⁵⁷ (<http://www.rcsb.org>, PDB ID: 4IB4), and the amino acid sequence of the target receptor was retrieved from the Universal Protein Resource⁵⁸ (UniProt IDs: P41595). The template was pre-processed as follows: after manual removal of the apocytochrome b₅₆₂ RIL (BRIL) fusion protein and co-crystallized ligand, water, and lipid molecules, ionization states of protein sidechains and hydrogen positions were assigned with the Protein Preparazion Wizard tool.⁵⁹ Prime 4.1⁶⁰ was used to build homology models (ClustalW alignment method and knowledge-based building method) and to reconstruct and refine missing loop domains except IL3 (Serial loop sampling, default level of accuracy). N-terminal and C-terminal portions were not modeled if their lengths exceeded those of the template. The C- and N-termini of the protein and the boundaries of missing IL3 were capped with acetyl and methylamino groups, respectively.

Induced Fit Docking—Compound **23** was docked to the homology model by means of the IFD procedure based on Glide search algorithm⁶¹ using the Standard Protocol (SP) and OPLS3 force field.⁶² The centroid of Asp^{3.33} residue was selected as center of the Glide grid (inner box side = 10 Å; outer box side = auto). The ligand was initially docked rigidly into the receptor by applying a scaling factor of 0.5 to both ligand and protein van der Waals (vdW) radii. Up to 20 poses were collected, and the sidechains of residues within 5 Å of the ligand were refined with Prime.⁶⁰ The ligand were re-docked into the newly generated receptor conformations with Glide⁶¹ by generating up to 10 poses using the SP scoring function and reverting the vdW radii scaling factors to their default values.

Molecular dynamics—The best obtained docking pose of **23** and the homology model of the apo receptor were subjected to 30 ns of membrane MD simulations. The structures were embedded in a 1-palmitoyl-2-oleoyl-sn-glycero-3-phosphocholine (POPC) lipid bilayer (80×80 Å wide, generated through the VMD⁶³ Membrane Plugin tool) according to the orientation suggested by the “Orientations of Proteins in Membranes (OPM)” server.⁶⁴ Overlapping lipids (within 0.6 Å) were removed upon protein insertion and the systems were solvated with TIP3P⁶⁵ water and neutralized by Na⁺/Cl⁻ counter-ions (final concentration 0.154 M). MD simulations with periodic boundaries conditions were carried out with the ACEMD program⁶⁶ using the CHARMM36^{67,68}/CGenFF(3.0.1)^{69,70} force fields for lipid and protein, and ligand atoms, respectively. Ligand parameters were obtained by analogy through the ParamChem service with no further optimization. After parameters validation, constrains were applied to the dihedral angles of the (N)-methanocarba ring to avoid unfeasible south ring puckering. The systems were equilibrated through a stepwise procedure: in the first stage, after 2500 cycles of conjugate-gradient minimization aimed at reducing steric clashes arising from the manual setup of the system, 10 ns of MD simulation

were performed in the NPT ensemble, restraining protein (and ligand) atoms by a force constant of 1 kcal/mol·Å². In the second stage, once water molecules diffused inside the protein cavity and the lipid bilayer reached equilibrium, the constraints on the ligand atoms were maintained whereas those on protein atoms were removed except for alpha carbon atoms (force constant = 0.5 kcal/mol·Å²) for other 10 ns. During the equilibration procedure, the temperature was maintained at 310 K using a Langevin thermostat with a low damping constant of 1 ps⁻¹, and the pressure was maintained at 1 atm using a Berendensen barostat. Bond lengths involving hydrogen atoms were constrained using the M-SHAKE⁷¹ algorithm with an integration timestep of 2 fs. The equilibrated systems were then subjected to 30 ns of unrestrained MD simulations (NVT ensemble, damping constant of 0.1 ps⁻¹). Long-range Coulomb interactions were handled using the particle mesh Ewald summation method (PME)⁷² with grid size rounded to the approximate integer value of cell wall dimensions. A non-bonded cutoff distance of 9 Å with a switching distance of 7.5 Å was used. The biophysical validity of the membrane-protein systems was assessed by measuring the average area per lipid headgroup (APL, Table S3) using Grid-MAT-MD.⁷³ The simulation on the **23**-h5HT_{2B}R were run in triplicate and selection of a representative trajectory was based upon the cumulative total Ligand-Protein interaction energy (IE_{tot}) expressed as the sum of van der Waals (IE_{vdW}) and electrostatic (IE_{ele}) contribution and computed at frames extracted every 50 ps with the mdenergy function implemented in VMD⁶⁰ exploiting NAMD 2.10.⁷⁴ From the IE_{tot} values so obtained, we computed the cumulative sum of ligand-protein IE_{tot} (hereby denoted as “dynamic scoring function”, DSF_{tot}) as follows:

$$DSF_{tot} = \sum_{i=1}^n IE_{tot}$$

and derived the slope values by fitting a linear function as previously reported.⁷⁵ The replica that returned the highest absolute slope value (Supporting Information, Table S1) was selected. IE versus simulation time graphs were generated with Gnuplot.⁷⁶

Docking of compounds 14, 25, 26, 27 and 35—The selected compounds were docked to the final **23**-h5HT_{2B} MD refined structure including all the selected water molecules (*w1-w9*) with Glide⁶¹ by generating up to 5 poses using both the SP and XP scoring functions. The centroid of **23** was selected as center of the Glide grid (inner box side = 10 Å; outer box side = 30 Å).

Supplementary Material

Refer to Web version on PubMed Central for supplementary material.

Acknowledgments

We thank Dr. John Lloyd and Dr. Noel Whittaker (NIDDK) for mass spectral determinations. This research was supported by the National Institutes of Health (Intramural Research Program of the NIDDK and R01HL077707). We thank Dr. Bryan L. Roth and Dr. X. P. Huang (Univ. North Carolina at Chapel Hill) and National Institute of Mental Health's Psychoactive Drug Screening Program (Contract # HHSN-271-2008-00025-C) for screening data.

Abbreviations

AR	adenosine receptor
cAMP	adenosine 3',5'-cyclic monophosphate
CHO	Chinese hamster ovary
CNS	central nervous system
CYP	cytochrome P450
DMEM	Dulbecco's modified Eagle medium
DMF	<i>N,N</i> -dimethylformamide
EL	extracellular loop
GPCR	G protein-coupled receptor
HEPES	2-[4-(2-hydroxyethyl)piperazin-1-yl]ethanesulfonic acid
HEK	human embryonic kidney
HRMS	high resolution mass spectroscopy
5HT	5-hydroxytryptamine
IFD	induced fit docking
NMR	nuclear magnetic resonance
PBS	phosphate buffered saline
PDSP	Psychoactive Drug Screening Program
RFU	relative fluorescence unit
SAR	structure-affinity relationship
TBAP	tetrabutylammonium dihydrogenphosphate
TEA	triethylamine
TM	transmembrane helix
tPSA	total polar surface area
TSPO	translocator protein
MW	molecular weight

References

1. Besnard J, Ruda GF, Setola V, Abecassis K, Rodriguiz RM, Huang XP, Norval S, Sassano MF, Shin AI, Webster LA, Simeons FR, Stojanovski L, Prat A, Seidah NG, Constam DB, Bickerton GR, Read

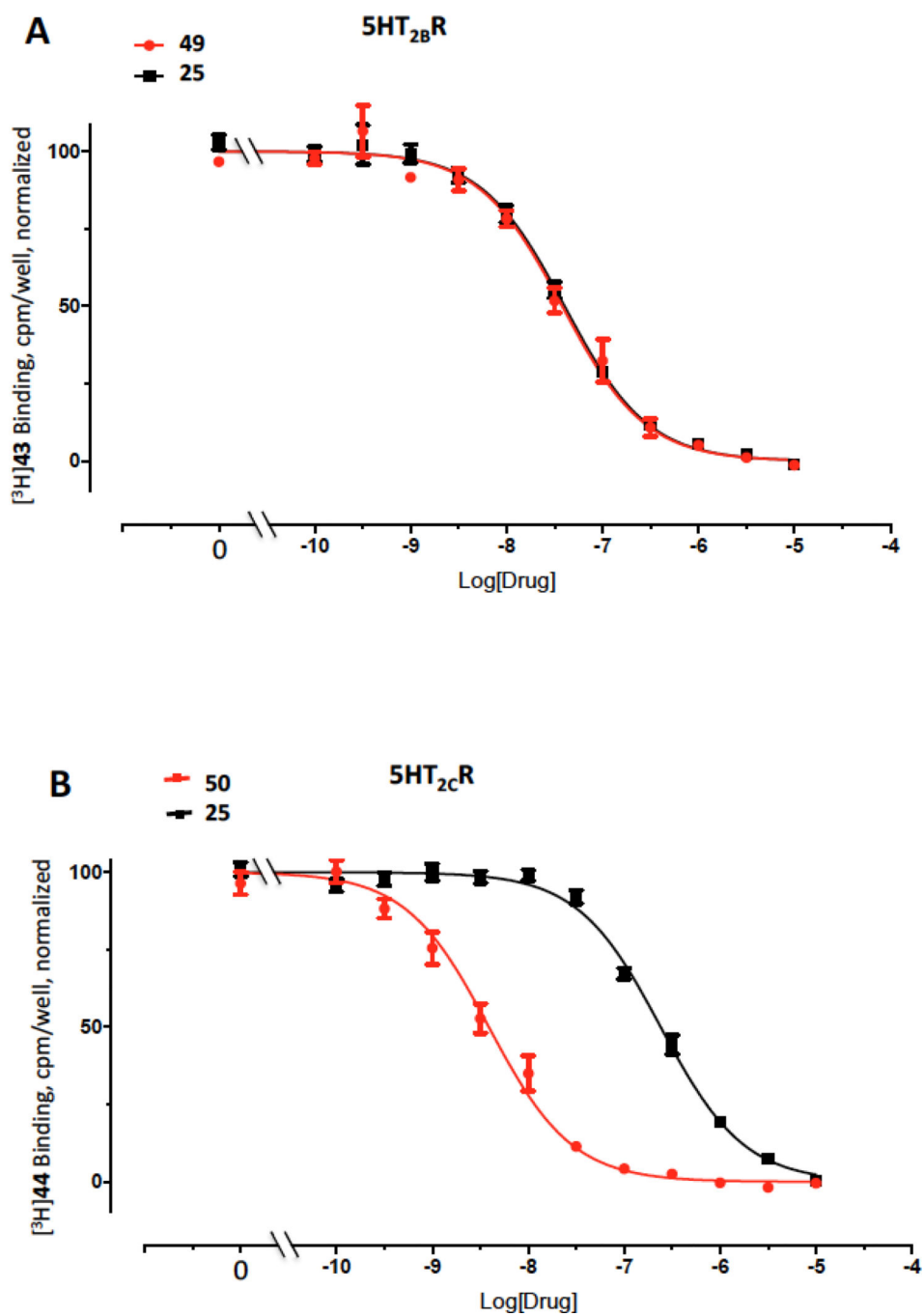
- KD, Wetsel WC, Gilbert IH, Roth BL, Hopkins AL. Automated design of ligands to polypharmacological profiles. *Nature*. 2012; 492:215–220. [PubMed: 23235874]
2. Jacobson KA, Costanzi S, Paoletta S. Computational studies to predict or explain GPCR polypharmacology. *Trends Pharmacol. Sci.* 2014; 35:658–663. [PubMed: 25458540]
 3. Chackalamannil S, Wang Y, Greenlee WJ, Hu Z, Xia Y, Ahn HS, Boykow G, Hsieh Y, Palamanda J, Agans-Fantuzzi J, Kurowski S, Graziano M, Chintala M. Discovery of a novel, orally active himbacine-based thrombin receptor antagonist (SCH 530348) with potent antiplatelet activity. *J. Med. Chem.* 2008; 51:3061–3064. [PubMed: 18447380]
 4. Patel G, Karver CE, Behera R, Guyett PJ, Sullenberger C, Edwards P, Roncal NE, Mensa-Wilmot K, Pollastri MP. Kinase scaffold repurposing for neglected disease drug discovery: discovery of an efficacious, lapatinib-derived lead compound for trypanosomiasis. *J. Med. Chem.* 2013; 56:3820–3832. [PubMed: 23597080]
 5. Jordheim LP, Durantel D, Zoulim F, Dumontet C. Advances in the development of nucleoside and nucleotide analogues for cancer and viral diseases. *Nat. Rev. Drug Discovery*. 2013; 12:447–464. [PubMed: 23722347]
 6. Triggle D. 1,4-Dihydropyridines as calcium channel ligands and privileged structures. *Cell. Mol. Neurobiol.* 2003; 23:293–303. [PubMed: 12825828]
 7. Welsch ME, Snyder SA, Stockwell BR. Privileged scaffolds for library design and drug discovery. *Curr. Opin. Chem. Biol.* 2010; 14:347–361. [PubMed: 20303320]
 8. Gallo-Rodriguez C, Ji X-D, Melman N, Siegman BD, Sanders LH, Orlina J, Fischer B, Pu Q-L, Olah ME, van Galen PJM, Stiles GL, Jacobson KA. Structure-activity relationships of N^6 -benzyladenosine-5'-uronamides as A_3 -selective adenosine agonists. *J. Med. Chem.* 1994; 37:636–646. [PubMed: 8126704]
 9. Paoletta S, Tosh DK, Salvemini D, Jacobson KA. Structural probing of off-target G protein-coupled receptor activities within a series of adenosine/adenine congeners. *PLoS ONE*. 2014; 9:e97858. [PubMed: 24859150]
 10. Ghosh E, Kumari P, Jaiman D, Shukla AK. Methodological advances: the unsung heroes of the GPCR structural revolution. *Nat. Rev. Mol. Cell Biol.* 2015; 16:69–81. [PubMed: 25589408]
 11. Chen JF, Eltzschig HK, Fredholm BB. Adenosine receptors as drug targets — what are the challenges? *Nat. Rev. Drug Discovery*. 2013; 12:265–286. [PubMed: 23535933]
 12. Diaz SL, Doly S, Narboux-Nême N, Fernández S, Mazot P, Banas SM, Boutourlinsky K, Moutkine I, Belmer A, Roumier A, Maroteaux L. 5-HT_{2B} receptors are required for serotonin-selective antidepressant actions. *Mol. Psychiatry*. 2012; 17:154–163. [PubMed: 22158014]
 13. Ebrahimkhani MR, Oakley F, Murphy LB, Mann J, Moles A, Perugorria MJ, Ellis E, Lakey AF, Burt AD, Douglass A, Wright MC, White SA, Jaffré F, Maroteaux L, Mann DA. Stimulating healthy tissue regeneration by targeting the 5-HT_{2B} receptor in chronic liver disease. *Nat. Med.* (N. Y., NY, U. S.). 2011; 17
 14. Janssen W, Schymura Y, Novoyatleva T, Kojonazarov B, Boehm M, Wietelmann A, Luitel H, Murmann K, Krompiec DR, Tretyn A, Pullamsetti S, Weissmann N, Seeger W, Ghofrani HA, Schermuly RT. 5-HT_{2B} Receptor antagonists inhibit fibrosis and protect from RV heart failure. *BioMed Res. Int.* 2015 Article ID 438403 <http://dx.doi.org/10.1155/2015/438403>.
 15. Roth BL. Drugs and valvular heart disease. *N. Engl. J. Med.* 2007; 356:6–9. [PubMed: 17202450]
 16. Mann DA, Oakley F. Serotonin paracrine signaling in tissue fibrosis. *Biochim. Biophys. Acta.* 2013; 1832:905–910. [PubMed: 23032152]
 17. Elangbam CS, Job LE, Zadrozny LM, Barton JC, Yoon LW, Gates LD, Slocum N. 5-Hydroxytryptamine (5HT)-induced valvulopathy: compositional valvular alterations are associated with 5HT_{2B} receptor and 5HT transporter transcript changes in Sprague-Dawley rats. *Exp. Toxicol. Pathol.* 2008; 60:253–262. [PubMed: 18511249]
 18. Zhou Y, Ma J, Lin X, Huang XP, Wu K, Huang N. Structure-based discovery of novel and selective 5-hydroxytryptamine 2B receptor antagonists for the treatment of irritable bowel syndrome. *J. Med. Chem.* 2016; 59:707–720. [PubMed: 26700945]
 19. Jazayeri A, Dias JM, Marshall FH. From G protein-coupled receptor structure resolution to rational drug design. *J. Biol. Chem.* 2015; 290:19489–19495. [PubMed: 26100628]

20. Tosh DK, Deflorian F, Phan K, Gao ZG, Wan TC, Gizewski E, Auchampach JA, Jacobson KA. Structure-guided design of A₃ adenosine receptor-selective nucleosides: Combination of 2-arylethynyl and bicyclo[3.1.0]hexane substitutions. *J. Med. Chem.* 2012; 55:4847–4860. [PubMed: 22559880]
21. Tosh DK, Paoletta S, Deflorian F, Phan K, Moss SM, Gao ZG, Jiang X, Jacobson KA. Structural sweet spot for A₁ adenosine receptor activation by truncated (N)-methanocarba nucleosides: Receptor docking and potent anticonvulsant activity. *J. Med. Chem.* 2012; 55:8075–8090. [PubMed: 22921089]
22. Tosh DK, Finley A, Paoletta S, Moss SM, Gao ZG, Gizewski E, Auchampach J, Salvemini D, Jacobson KA. In vivo phenotypic screening for treating chronic neuropathic pain: Modification of C2-arylethynyl group of conformationally constrained A₃ adenosine receptor agonists. *J. Med. Chem.* 2014; 57:9901–9914. [PubMed: 25422861]
23. Tosh DK, Paoletta S, Chen Z, Crane S, Lloyd J, Gao ZG, Gizewski E, Auchampach JA, Salvemini D, Jacobson KA. Structure-based design, synthesis by click chemistry and in vivo activity of highly selective A₃ adenosine receptor agonists. *Med. Chem. Comm.* 2015; 6:555–563.
24. Tosh DK, Crane S, Chen Z, Paoletta S, Gao ZG, Gizewski E, Auchampach JA, Salvemini D, Jacobson KA. Rigidified A₃ adenosine receptor agonists: 1-Deaza modification maintains high in vivo efficacy. *ACS Med. Chem. Lett.* 2015; 6:804–808. [PubMed: 26191370]
25. Gao ZG, Blaustein J, Gross AS, Melman N, Jacobson KA. N⁶-Substituted adenosine derivatives: Selectivity, efficacy, and species differences at A₃ adenosine receptors. *Biochem. Pharmacol.* 2003; 65:1675–1684. [PubMed: 12754103]
26. Lee K, Ravi RG, Ji XD, Marquez VE, Jacobson KA. Ring-constrained (N)methanocarba-nucleosides as adenosine receptor agonists: Independent 5'-uronamide and 2'-deoxy modifications. *Bioorg. Med. Chem. Lett.* 2001; 11:1333–1337. [PubMed: 11392549]
27. Melman A, Gao ZG, Kumar D, Wan TC, Gizewski E, Auchampach JA, Jacobson KA. Design of (N)-methanocarba adenosine 5'-uronamides as species-independent A₃ receptor-selective agonists. *Bioorg. Med. Chem. Lett.* 2008; 18:2813–2819. [PubMed: 18424135]
28. Tosh DK, Padia J, Salvemini D, Jacobson KA. Efficient, large-scale synthesis and preclinical studies of MRS5698, a highly selective A₃ adenosine receptor agonist that protects against chronic neuropathic pain. *Purinergic Signalling.* 2015; 11:371–387. [PubMed: 26111639]
29. Joshi BV, Melman A, Mackman RL, Jacobson KA. Synthesis of ethyl (1*S*,2*R*,3*S*,4*S*,5*S*)-2,3-*O*-(isopropylidene)-4-hydroxy-bicyclo[3.1.0]hexane-carboxylate from L-ribose: A versatile chiral synthon for preparation of adenosine and P2 receptor ligands. *Nucleosides Nucleotides Nucleic Acids.* 2008; 27:279–291. [PubMed: 18260011]
30. Fishman P, Bar-Yehuda S, Liang BT, Jacobson KA. Pharmacological and therapeutic effects of A₃ adenosine receptor (A₃AR) agonists. *Drug Discovery Today.* 2012; 17:359–366. [PubMed: 22033198]
31. Jacobson KA, Ohno M, Duong HT, Kim SK, Tchilibon S, Cesnek M, Holy A, Gao ZG. A neoceptor approach to unraveling microscopic interactions between the human A_{2A} adenosine receptor and its agonists. *Chem. Biol. (Oxford, U. K.).* 2005; 12:237–247.
32. Wacker D, Wang C, Katritch V, Han GW, Huang XP, Vardy E, McCorvy JD, Jiang Y, Chu M, Siu FY, Liu W, Xu HE, Cherezov V, Roth BL, Stevens RC. Structural features for functional selectivity at serotonin receptors. *Science.* 2013; 340:615–619. [PubMed: 23519215]
33. Tosh DK, Paoletta S, Chen Z, Moss SM, Gao Z-G, Salvemini D, Jacobson KA. Extended N⁶ substitution of rigid C2-arylethynyl nucleosides for exploring the role of extracellular loops in ligand recognition at the A₃ adenosine receptor. *Bioorg. Med. Chem. Lett.* 2014; 24:3302–3306. [PubMed: 24969016]
34. Rasmussen SGF, DeVree BT, Zou Y, Kruse AC, Chung KY, Kobilka TS, Thian FS, Chae PS, Pardon E, Calinski D, Mathiesen JM, Shah STA, Lyons JA, Caffrey M, Gellman SH, Steyaert J, Skinotis G, Weis WI, Sunahara RK, Kobilka BK. Crystal structure of the beta2 adrenergic receptor-Gs protein complex. *Nature.* 2011; 477:549–555. [PubMed: 21772288]
35. Cherezov V, Rosenbaum DM, Hanson MA, Rasmussen SGF, Thian FS, Kobilka TS, Choi H-J, Kuhn P, Weis WI, Kobilka BK, Stevens RC. High-resolution crystal structure of an engineered human beta2-adrenergic G protein-coupled receptor. *Science.* 2007; 318:1258–1265. [PubMed: 17962520]

36. Martí-Solano M, Sanz F, Pastor M, Selent J. A dynamic view of molecular switch behavior at serotonin receptors: Implications for Functional selectivity. *PLoS ONE*. 2014; 9:e109312. [PubMed: 25313636]
37. Venkatakrishnan AJ, Deupi X, Lebon G, Tate CG, Schertler GF, Babu MM. Molecular signatures of G-protein-coupled receptors. *Nature*. 2013; 494:185–194. [PubMed: 23407534]
38. Isberg V, de Graaf C, Bortolato A, Cherezov V, Katritch V, Marshall F, Mordalski S, Pin J-P, Stevens RC, Vriend G, Gloriam DE. Generic GPCR residue numbers - aligning topology maps while minding the gaps. *Trends Pharmacol. Sci.* 2015; 36:22–31. [PubMed: 25541108]
39. Liu W, Wacker D, Gati C, Han GW, James D, Wang D, Nelson G, Weierstall U, Katritch V, Barty A, Zatsepin NA, Li D, Messerschmidt M, Boutet S, Williams GJ, Koglin JE, Seibert MM, Wang C, Shah ST, Basu S, Fromme R, Kupitz C, Rendek KN, Grotjohann I, Fromme P, Kirian RA, Beyerlein KR, White TA, Chapman HN, Caffrey M, Spence JC, Stevens RC, Cherezov V. Serial femtosecond crystallography of G protein-coupled receptors. *Science*. 2013; 342:1521–1524. [PubMed: 24357322]
40. West JD, Carrier EJ, Bloodworth NC, Schroer AK, Chen P, Ryzhova LM, Gladson S, Shay S, Hutcheson JD, Merryman WD. Serotonin 2B receptor antagonism prevents heritable pulmonary arterial hypertension. *PLoS One*. 2016; 11:e0148657. [PubMed: 26863209]
41. Morita H, Mochiki E, Takahashi N, Kawamura K, Watanabe A, Sutou T, Ogawa A, Yanai M, Ogata K, Fujii T, Ohno T, Tsutsumi S, Asao T, Kuwano H. Effects of 5-HT_{2B}, 5-HT₃ and 5-HT₄ receptor antagonists on gastrointestinal motor activity in dogs. *World J. Gastroenterol.* 2013; 19:6604–6612. [PubMed: 24151388]
42. Rodrigues T, Hauser N, Reker D, Reutlinger M, Wunderlin T, Hamon J, Koch G, Schneider G. Multidimensional de novo design reveals 5-HT_{2B} receptor-selective ligands. *Angew. Chem. Int. Ed.* 2015; 54:1551–1555.
43. Kwon YJ, Saubern S, Macdonald JM, Huang XP, Setola V, Roth BL. N-Tetrahydrothiochromenoisoxazole-1-carboxamides as selective antagonists of cloned human 5-HT_{2B}. *Bioorg. Med. Chem. Lett.* 2010; 20:5488–5490. [PubMed: 20692833]
44. Moss N, Choi Y, Cogan D, Flegg A, Kahrs A, Loke P, Meyn O, Nagaraja R, Napier S, Parker A, Peterson JT, Ramsden P, Sarko C, Skow D, Tomlinson J, Tye H, Whitaker M. A new class of 5-HT_{2B} antagonists possesses favorable potency, selectivity, and rat pharmacokinetic properties. *Bioorg. Med. Chem. Lett.* 2009; 19:2206–2210. [PubMed: 19307114]
45. González-Maeso J, Weisstaub NV, Zhou M, Chan P, Ivic L, Ang R, Lira A, Bradley-Moore M, Ge Y, Zhou Q, Sealfon SC, Gingrich JA. Hallucinogens recruit specific cortical 5-HT_{2A} receptor-mediated signaling pathways to affect behavior. *Neuron*. 2007; 53:439–452. (2007). [PubMed: 17270739]
46. Kamal M, Gbahou F, Guillaume JL, Daulat AM, Benleulmi-Chaachoua A, Luka M, Chen P, Kalbasi Anaraki D, Baroncini M, Mannoury la Cour C, Millan MJ, Prevot V, Delagrangre P, Jockers R. Convergence of melatonin and serotonin (5-HT) signaling at MT₂/5-HT_{2C} receptor heteromers. *J. Biol. Chem.* 2015; 290:11537–11546. [PubMed: 25770211]
47. Wei F, Gu M, Chu YX. New tricks for an old slug: Descending serotonergic system in pain. *Shengli Xuebao*. 2012; 64:520–530.
48. Urtikova N, Berson N, Van Steenwinkel J, Doly S, Truchetto J, Maroteaux L, Pohl M, Conrath M. Antinociceptive effect of peripheral serotonin 5-HT_{2B} receptor activation on neuropathic pain. *Pain*. 2012; 153:1320–1331. [PubMed: 22525520]
49. Janes K, Symons-Liguori AM, Jacobson KA, Salvemini D. Identification of A₃ adenosine receptor agonists as novel non-narcotic analgesics. *Br. J. Pharmacol.* 2016; 173:1253–1267. [PubMed: 26804983]
50. Schaddelee MP, Read KD, Cleypool CG, IJzerman AP, Danhof M, de Boer AG. Brain penetration of synthetic adenosine A₁ receptor agonists in situ: role of the rENT1 nucleoside transporter and binding to blood constituents. *Eur. J. Pharm. Sci.* 2005; 24:59–66. [PubMed: 15626578]
51. Chanrion B, Mannoury la Cour C, Gavarini S, Seimandi M, Vincent L, Pujol JF, Bockaert J, Marin P, Millan MJ. Inverse agonist and neutral antagonist actions of antidepressants at recombinant and native 5-hydroxytryptamine_{2C} receptors: differential modulation of cell surface expression and signal transduction. *Mol. Pharmacol.* 2008; 73:748–757. [PubMed: 18083778]

52. Carman AJ, Mills JH, Krenz A, Kim DG, Bynoe MS. Adenosine receptor signaling modulates permeability of the blood–brain barrier. *J. Neurosci.* 2011; 31:13272–13280. [PubMed: 21917810]
53. Cheng YC, Prusoff WH. Relationship between inhibition constant (K₁) and concentration of inhibitor which causes 50 percent inhibition (I₅₀) of an enzymatic-reaction. *Biochem. Pharmacol.* 1973; 22:3099–3108. [PubMed: 4202581]
54. Roth BL, Craigo SC, Choudhary MS, Uluer A, Monsma FJ, Shen Y, Meltzer HY, Sibley DR. Binding of typical and atypical antipsychotic agents to 5-hydroxytryptamine-6 and 5-hydroxytryptamine-7 receptors. *J. Pharmacol. Exp. Ther.* 1994; 268:1403–1410. [PubMed: 7908055]
55. Maestro, version 10.3. New York, NY: Schrödinger, LLC; 2015.
56. Jaguar, version 8.9. New York, NY: Schrödinger, LLC; 2015.
57. Bernstein FC, Koetzle TF, Williams GJ, Meyer EE Jr, Brice MD, Rodgers JR, Kennard O, Shimanouchi T, Tasumi M. The Protein Data Bank: A computer-based archival file for macromolecular structures. *J. Mol. Biol.* 1977; 112:535–542. [PubMed: 875032]
58. The UniProt Consortium. UniProt: a hub for protein information. *Nucleic Acids Res.* 2015; 43:D204–D212. [PubMed: 25348405]
59. Sastry GM, Adzhigirey M, Day T, Annabhimoju R, Sherman W. Protein and ligand preparation: parameters, protocols, and influence on virtual screening enrichments. *J. Comput. Aided Mol. Des.* 2013; 27:221–234. [PubMed: 23579614]
60. Prime, version 4.1. New York, NY: Schrödinger, LLC; 2015.
61. Glide, version 6.8. New York, NY: Schrödinger, LLC; 2015.
62. Harder E, Damm W, Maple J, Wu C, Reboul M, Xiang JY, Wang L, Lupyan D, Dahlgren MK, Knight JL, Kaus JW, Cerutti DS, Krilov G, Jorgensen WL, Abel R, Friesner RA. OPLS3: A force field providing broad coverage of drug-like small molecules and proteins. *J. Chem. Theory Comput.* 2016; 12:281–296. [PubMed: 26584231]
63. Humphrey W, Dalke A, Schulten K. VMD - Visual molecular dynamics. *J. Mol. Graphics.* 1996; 14:33–38.
64. Lomize MA, Pogozheva ID, Joo H, Mosberg HI, Lomize AL. OPM database and PPM web server: resources for positioning of proteins in membranes. *Nucleic Acids Res.* 2012; 40:D370–D376. [PubMed: 21890895]
65. Jorgensen WL, Chandrasekhar J, Madura JD, Impey RW, Klein ML. Comparison of simple potential functions for simulating liquid water. *J. Chem. Phys.* 1983; 79:926–935.
66. Harvey M, Giupponi G, De Fabritiis G. ACEMD: Accelerated molecular dynamics simulations in the microseconds timescale. *J. Chem. Theory Comput.* 2009; 5:1632–1639. [PubMed: 26609855]
67. Best RB, Zhu X, Shim J, Lopes PEM, Mittal J, Feig M, MacKerell AD Jr. Optimization of the additive CHARMM all-atom protein force field targeting improved sampling of the backbone phi, psi and side-chain chi₁ and chi₂ dihedral angles. *J. Chem. Theory Comput.* 2012; 8:3257–3273. [PubMed: 23341755]
68. Klauda JB, Venable RM, Freites JA, O'Connor JW, Tobias DJ, Mondragon-Ramirez C, Vorobyov I, MacKerell AD Jr, Pastor RW. Update of the CHARMM all-atom additive force field for lipids: validation on six lipid types. *J. Phys. Chem. B.* 2010; 114:7830–7843. [PubMed: 20496934]
69. Vanommeslaeghe K, MacKerell AD Jr. Automation of the CHARMM General Force Field (CGenFF) I: bond perception and atom typing. *J. Chem. Inf. Model.* 2012; 52:3144–3154. [PubMed: 23146088]
70. Vanommeslaeghe K, Raman EP, MacKerell AD Jr. Automation of the CHARMM General Force Field (CGenFF) II: assignment of bonded parameters and partial atomic charges. *J. Chem. Inf. Model.* 2012; 52:3155–3168. [PubMed: 23145473]
71. Krätzler V, Van Gunsteren WF, Hünenberger PH. A Fast SHAKE algorithm to solve distance constraint equations for small molecules in molecular dynamics simulations. *J. Comput. Chem.* 2001; 22:501–508.
72. Essmann U, Perera L, Berkowitz ML, Darden T, Lee H, Pedersen LGA. Smooth particle mesh Ewald method. *J. Chem. Phys.* 1995; 103:8577–8593.
73. Allen WJ, Lemkul JA, Bevan DR. GridMAT-MD: A grid-based membrane analysis tool for use with molecular dynamics. *J. Comput. Chem.* 2009; 30:1952–1958. [PubMed: 19090582]

74. Phillips JC, Braun R, Wang W, Gumbart J, Tajkhorshid E, Villa E, Chipot C, Skeel RD, Kale L, Schulten K. Scalable molecular dynamics with NAMD. *J. Comput. Chem.* 2005; 26:1781–1802. [PubMed: 16222654]
75. Sabbadin D, Ciancetta A, Moro S. Bridging molecular docking to membrane molecular dynamics to investigate GPCR–ligand recognition: The human A_{2A} adenosine receptor as a key study. *J. Chem. Inf. Model.* 2014; 54:169–183. [PubMed: 24359090]
76. Williams T, Kelley C. Gnuplot 4.6: An Interactive Plotting Program, version 4.6.6. 2014 [accessed September 27, 2016] [Online]; <http://gnuplot.info>.
77. Carlin JL, Tosh DK, Xiao C, Piñol RA, Chen Z, Salvemini D, Gavrilova O, Jacobson KA, Reitman ML. Peripheral adenosine A₃ receptor activation causes regulated hypothermia in mice that is dependent on central histamine H₁ receptors. *J. Pharmacol. Exp. Ther.* 2016; 356:474–482. [PubMed: 26606937]



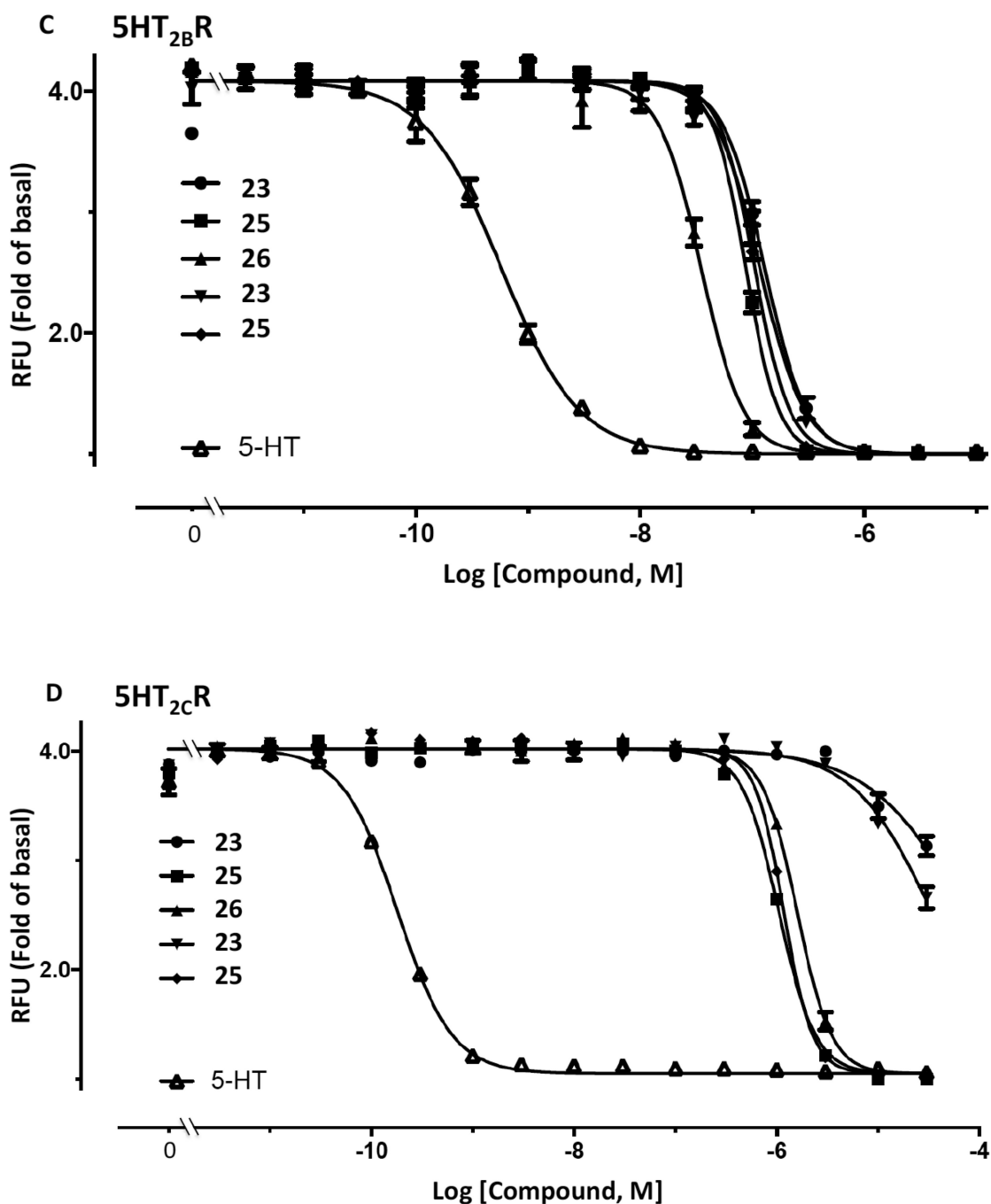


Figure 1.

Representative binding curves at the (A) 5HT_{2B}R and (B) 5HT_{2C}R for compound **25** (black curves), in comparison to reference compounds (red curves): (A) 3,5-dihydro-5-methyl-*N*-3-pyridinylbenzo[1,2-*b*:4,5-*b'*]dipyrrole-1(2*H*)-carboxamide (**49**, SB206553) and (B) 6-[2-[4-[bis(4-fluorophenyl)methylene]-1-piperidinyl]ethyl]-7-methyl-5*H*-thiazolo[3,2-*a*]pyrimidin-5-one (**50**, ritanserin). Radioligands used were: 5HT_{2B}R, binding with [³H]lysergic acid diethylamide **43**; 5HT_{2C}R, binding with [³H]mesulergine **44**. Representative functional assays at the (C) 5HT_{2B}R and (D) 5HT_{2C}R for compounds **23**, **25**

and **26**, in comparison to reference compound 5-HT applied to desensitize the response. 5-HT (3 nM, EC₈₀) was used as an agonist in both C and D. Compound **26** (10 μM) did not display significant agonist or antagonist activity (>10%) at the 5HT_{2A}R or agonist activity at 5HT_{2B}R or 5HT_{2C}R (data not shown). RFU, relative fluorescence units. Mean ± s.e.m. is shown (n = 3). The curves for all compounds were best fit using a monophasic isotherm with a variable Hill slope (F-test, *P* < 0.05 was considered as statistically significant).

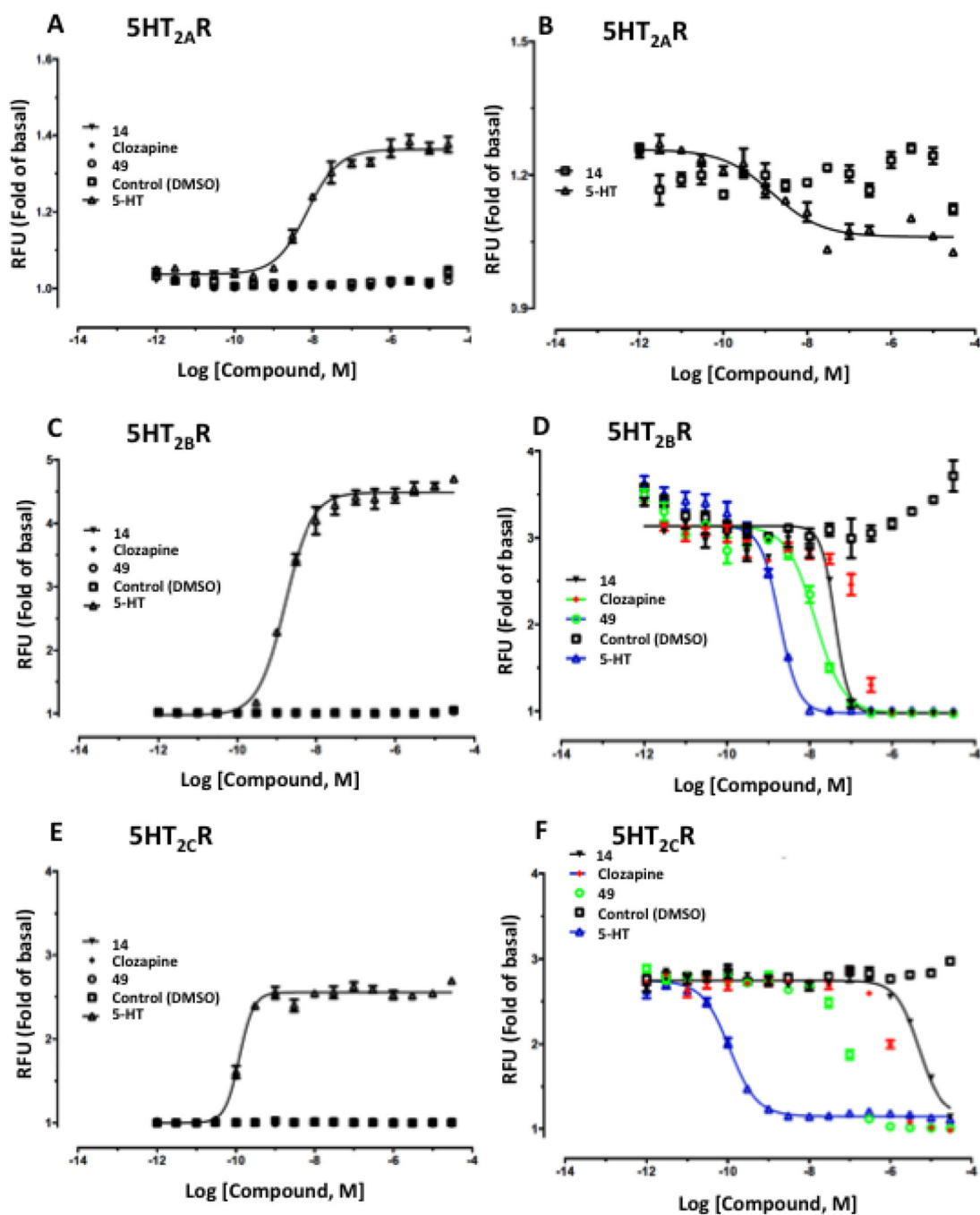


Figure 2. Representative functional assays at the (A, B) 5HT_{2A}R, (C, D) 5HT_{2B}R and (D, E) 5HT_{2C}R for compound 14, in comparison to reference compound 5-HT applied to desensitize the response. 5-HT (3 nM, EC₈₀) was used as agonist in B, D and F. RFU, relative fluorescence units.

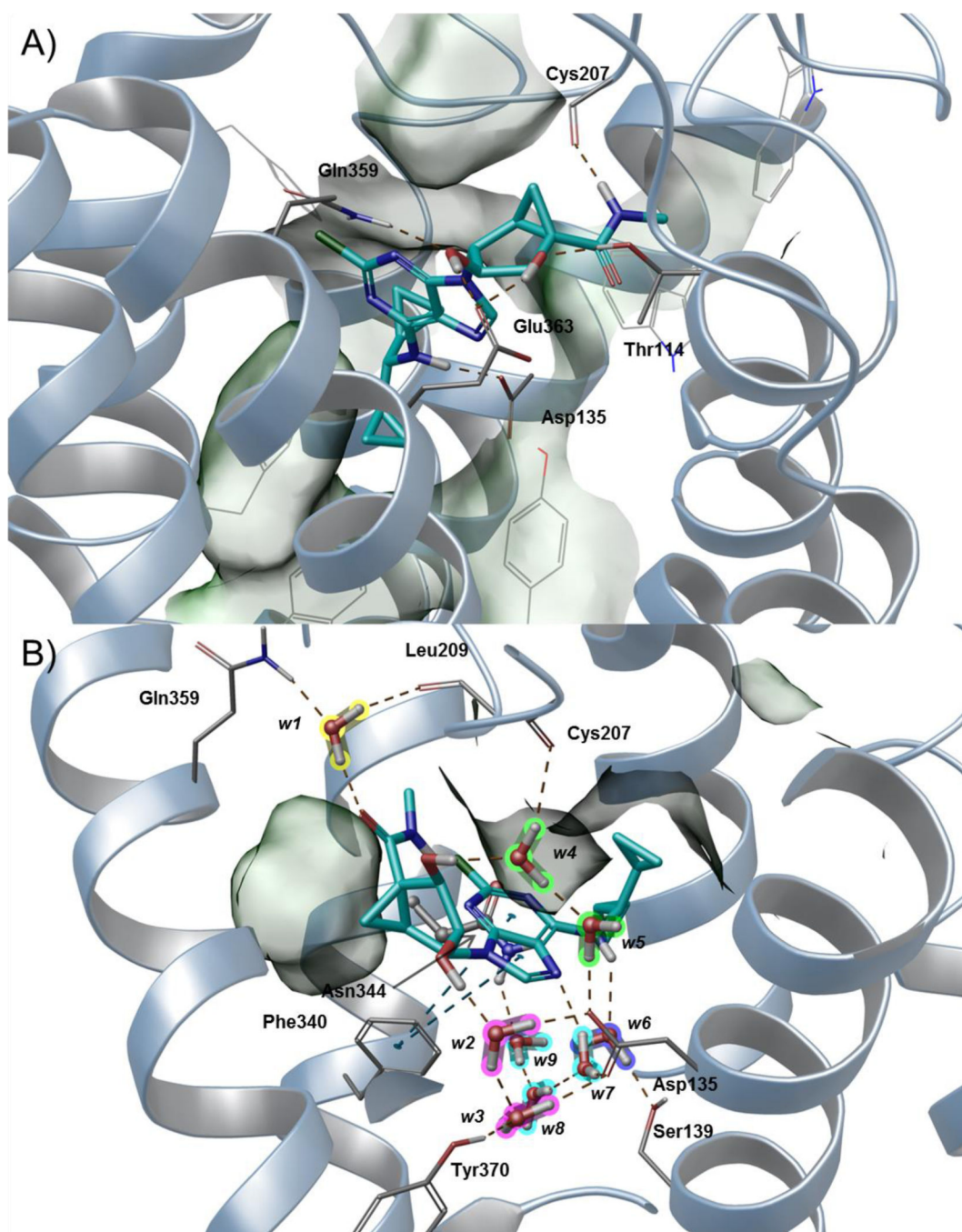


Figure 3. Hypothetical binding modes predicted by IFD (A) and following MD (B) simulation of *N*⁶-dicyclopropylmethyl 5'-methylamide (*N*)-methanocarpa derivative **23** (cyan carbon atoms, sticks representation) at the h5HT_{2B}R. Side chains of residues important for ligand recognition (grey carbon atoms) and water molecules (highlighted with different colors according to the ligand moiety they interact with) are reported as sticks. Residues establishing hydrophobic contacts with the ligand are depicted also as transparent surfaces. H-bonds and π - π stacking interactions are pictured as dashed yellow and cyan lines,

respectively. Nonpolar hydrogen atoms are omitted. Helices are shown as ribbon structures numbered (from right to left) in A, TMs 1, 2, 3, 4, 5, 6 and 7, and in B, TMs 3, 4, 5, 6 and 7.

Author Manuscript

Author Manuscript

Author Manuscript

Author Manuscript

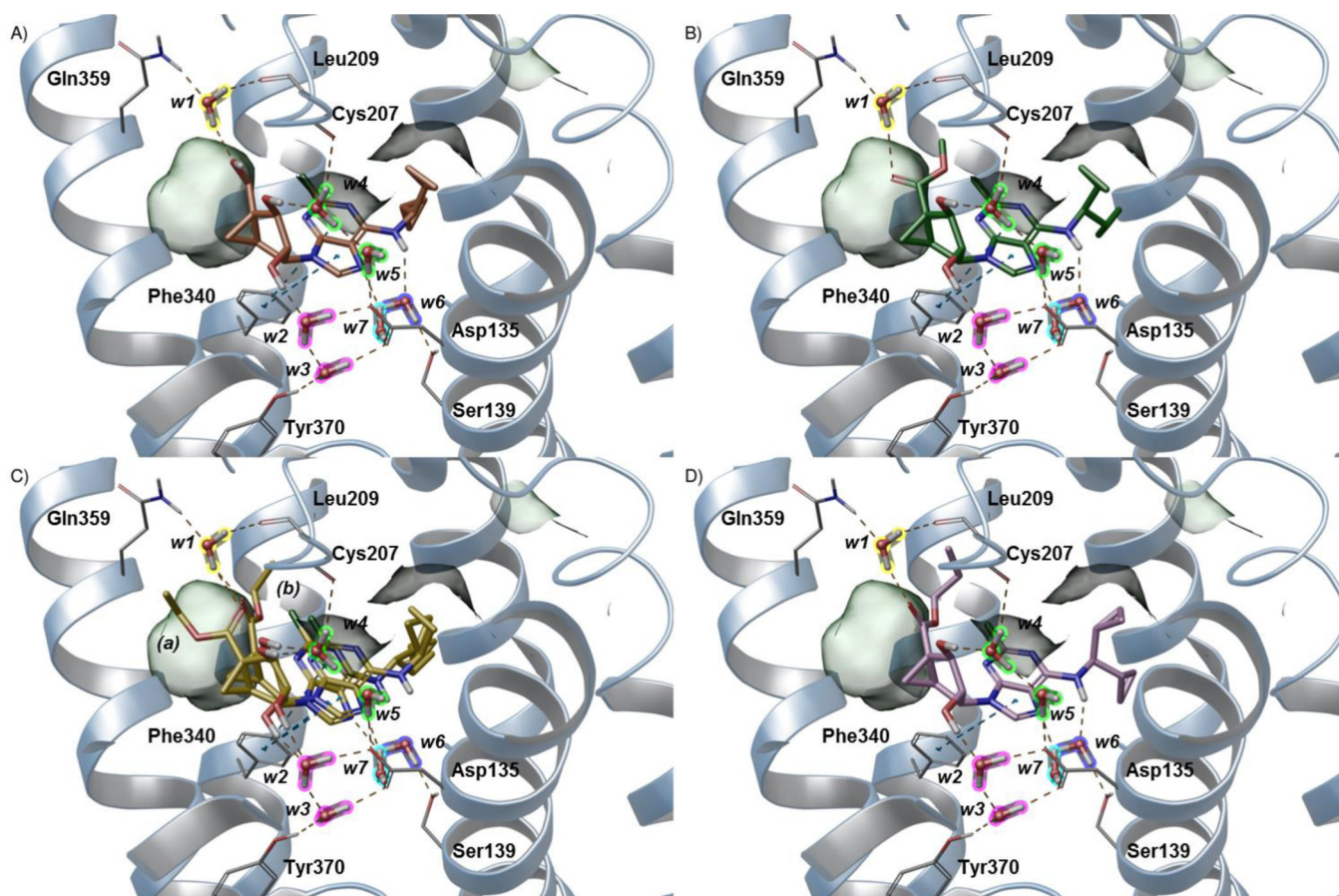
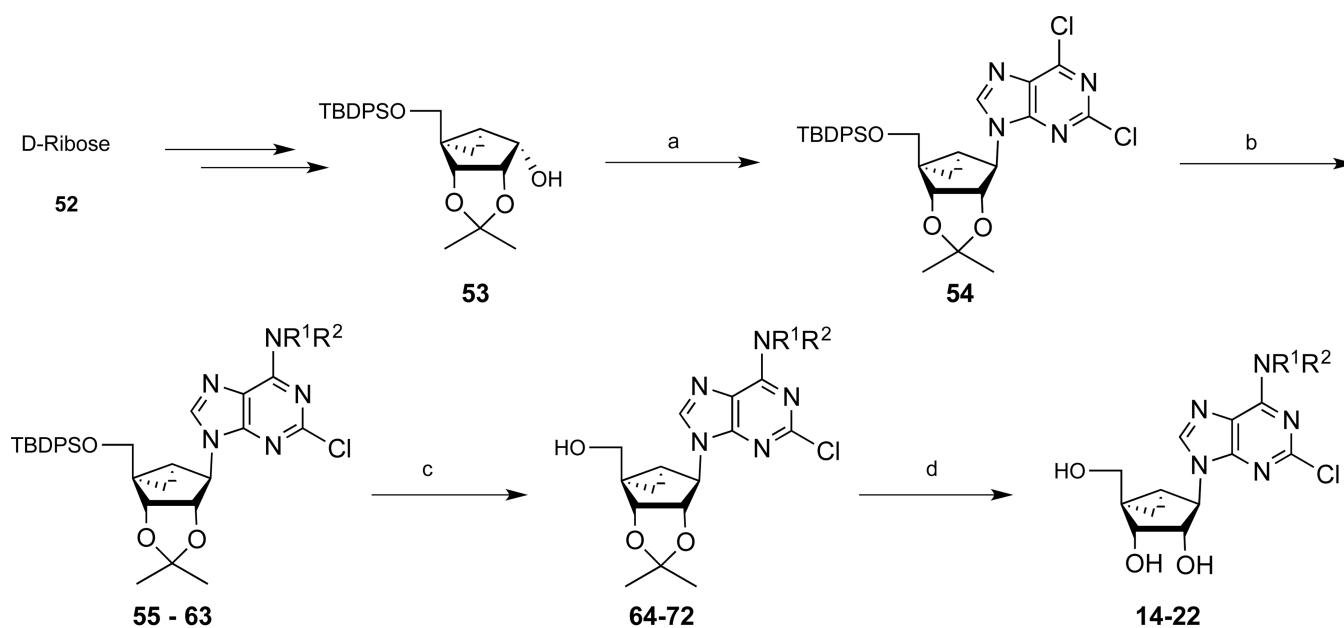


Figure 4.

Hypothetical binding mode predicted by rigid docking at the h5HT_{2B}R (including all water molecules) for *N*⁶-dicyclopropylmethyl (*N*)-methanocarpa derivatives bearing different 5'-groups: A) **14** (5'-hydroxy, orange carbon atoms); B) **25** (5'-methyl ester, green carbon atoms); C) **26** (5'-ethyl ester, yellow carbon atoms, two alternative binding modes are reported); and D) **27** (5'-propyl ester, pink carbon atoms). Side chains of residues important for ligand recognition (grey carbon atoms) and water molecules (highlighted with different colors according to the ligand moiety they interact with) are represented as sticks. Residues establishing hydrophobic contacts with the ligand are also depicted as transparent surfaces. H-bonds and π - π stacking interactions are pictured as dashed yellow and cyan lines, respectively. Nonpolar hydrogen atoms, the sidechain of Asn344^{6,55} and *w8* and *w9* are omitted to aid visualization.



55, 64, 14; R¹=H, R²=dicyclopropylCH

56, 65, 15; R¹=H, R²=diethylCH

57, 66, 16; R¹=H, R²=(*R*)-cyclopropylethylCH

58, 67, 17; R¹=H, R²=(*S*)-cyclopropylethylCH

59, 68, 18; R¹=H, R²=(*R*)-cyclopropylisopropylCH

60, 69, 19; R¹=H, R²=(*S*)-cyclopropylisopropylCH

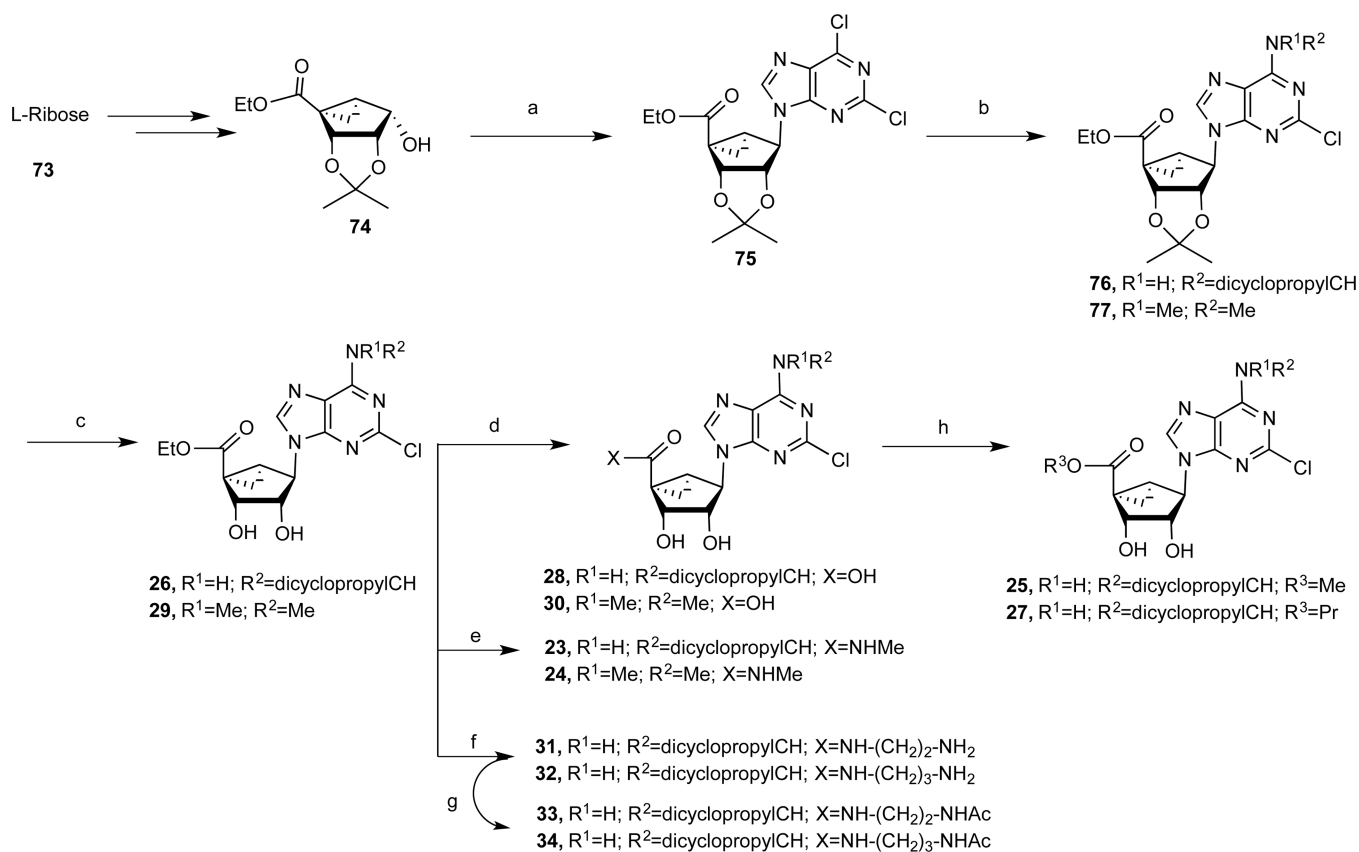
61, 70, 20; R¹=H, R²=(*S*)-cyclopropylcyclobutylCH

62, 71, 21; R¹=H, R²=(*R*)-cyclopropylcyclobutylCH

63, 72, 22; R¹=Me, R²=Me

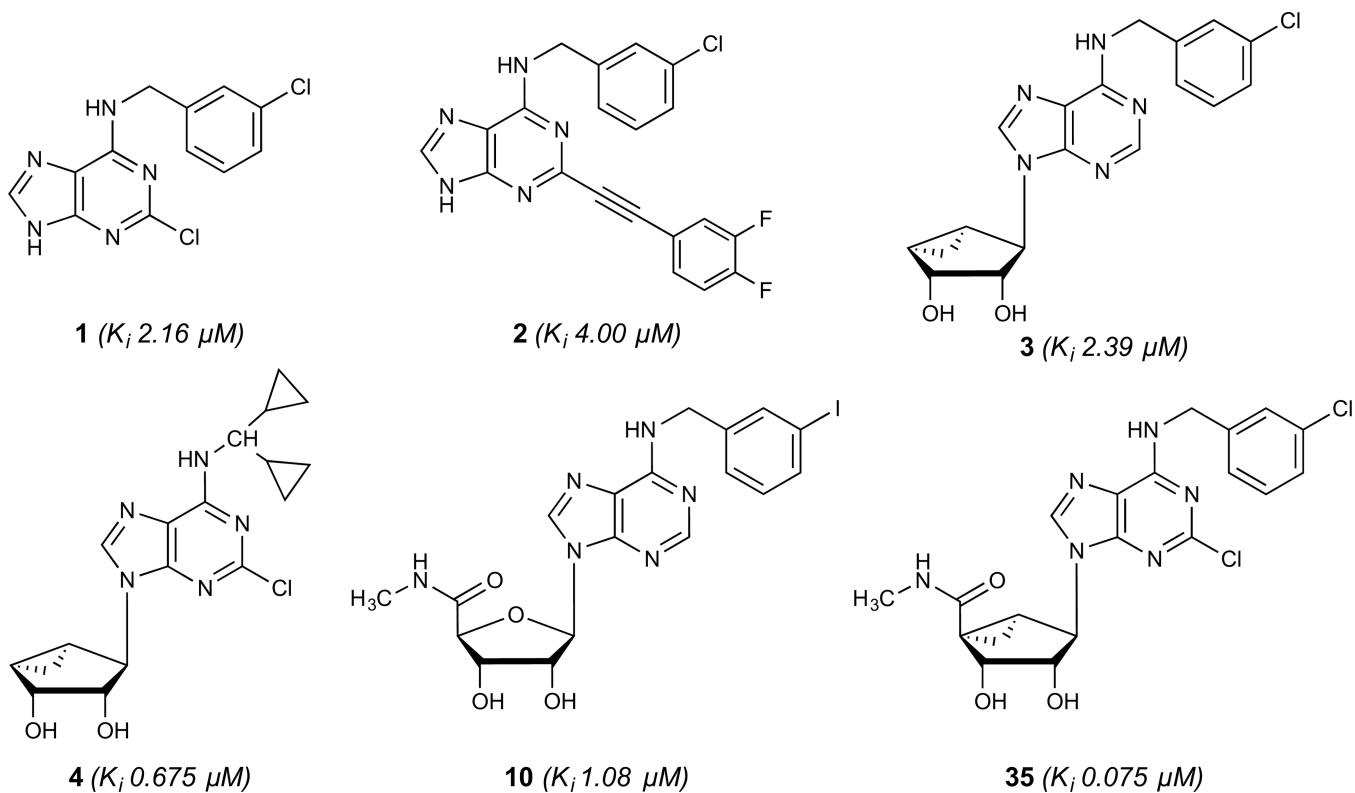
Scheme 1.

Synthesis of *N*⁶-alkyl-(*N*)-methanocarba-adenosine (5'-OH) derivatives. Reagents: (a) 2,6-dichloropurine, Ph₃P, DIAD, THF, rt, 69%; (b) RNH₂, Et₃N, MeOH, rt, 78–85%; (c) TBAF, THF, rt, 68–80%; (d) Dowex50, MeOH-H₂O, 67–85%. All steps were performed at rt. Compound **22** was prepared from **63** without isolation of protected intermediate.



Scheme 2.

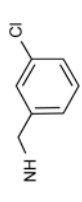
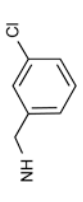
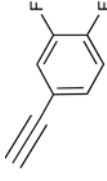
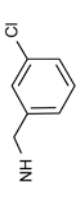
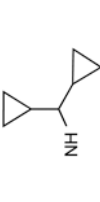
Synthesis of N^6 -alkyl-(N)-methanocarpa-adenosine (4'-carbonyl) derivatives. Reagents and Condition: (a) 2,6-dichloropurine, Ph_3P , DIAD, THF, rt; (b) RNH_2 , Et_3N , MeOH, rt, 85–87%; (c) Dowex50, MeOH- H_2O , rt, 86–88%; (d) 1N NaOH, MeOH, rt, 76–77%; (e) 40% $MeNH_2$, MeOH, rt, 65–67%; (f) $H_2N(CH_2)_nNH_2$, MeOH, rt, 63–64%; (g) 2,5-dioxo-2,5-dihydro-1*H*-pyrrol-1-yl acetate, Et_3N , DMF, rt, 58–59%; (h) ROH, DMAP, DCC, DMF, rt.

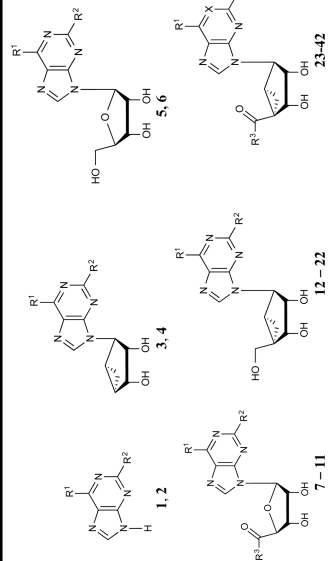
**Chart 1.**


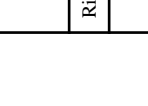

Adenine (**1**, **2**), nucleoside (**10**) and (N)-methanocarba nucleoside (**3**, **4**, **31**) derivatives that were previously reported to interact with the 5HT_{2B}R (binding *K_i* values are shown in italics).⁹

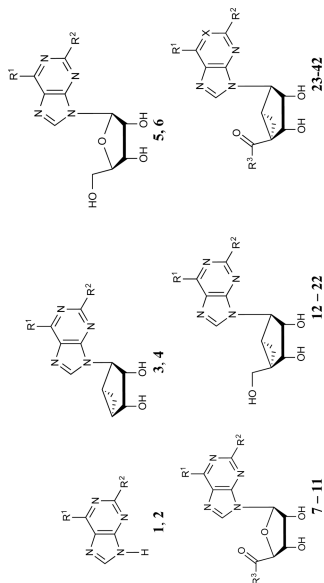
Table 1

Structures and binding affinities of nucleoside derivatives at 5HT₂Rs and at A₁ and A₃ARs, including newly synthesized (14–34, 42) derivatives and previously reported (1–13, 35–41) nucleosides. R³ = NHCH₃ and X = N, unless noted. Human (h) ARs, unless noted (r = rat).

No.	R ¹	R ²	5HT _{2A} R % inhibition or K _i (μM) ^a	5HT _{2B} R % inhibition or K _i (μM) ^a	5HT _{2C} R % inhibition or K _i (μM) ^a	A ₁ AR, % inhibition or K _i (μM) ^b	A _{2A} AR, % inhibition or K _i (μM) ^b	A ₃ AR, % inhibition or K _i (μM) ^b
Ademine and truncated nucleoside derivatives								
1 ^b		Cl	26%	2.16± 0.045	3.35± 0.34	45%	37%	0.165
2 ^b			<10%	4.00± 1.36	11%	<10%	<10%	0.120
3 ^b		Cl	<10%	2.39± 0.55	4.10± 1.62	1.6	4.52	4.9
4 ^b		Cl	<10%	0.675± 0.100	1.86± 0.22	0.048	3.95	0.47




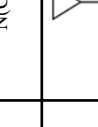


No.	R ¹	R ²	5HT _{2A} R inhibition or K _i (μM) ^a	5HT _{2B} R inhibition or K _i (μM) ^a	5HT _{2C} R inhibition or K _i (μM) ^a	A ₁ AR, % inhibition or K _i (μM) ^b	A _{2A} AR, % inhibition or K _i (μM) ^b	A _{2B} AR, % inhibition or K _i (μM) ^b
Riboside 5'-OH derivatives								
5	NH ₂	Cl	46%	<10%	<10%	0.0028	0.063 (r) ^c	0.087 ^c
6		H	<10%	38%	11%	0.0008 (r) ^b	1.37 (r) ^c	0.041 ^c
Riboside 5'-N-alkylamide derivatives								
7	NH ₂	H	<10%	<10%	<10%	0.084 (r) ^c	0.0668 (r) ^c	0.072 (r) ^c
8	NH ₂	H	<10%	<10%	<10%	0.0068	0.0103 (r) ^b	0.016
9	NH ₂	H	<10%	<10%	<10%	0.013 (r) ^c	0.0134 (r) ^c	1.6 (r) ^c
10		H	<10%	1.08	5.42	0.70	6.20	0.0017 ^c
11		Cl	~30%	2.77±0.56	~10	0.22	5.40	0.0014 ^c

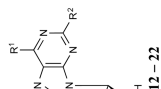
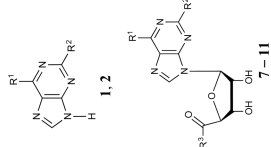
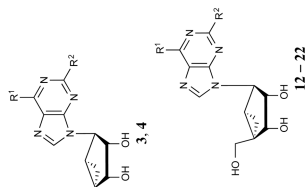
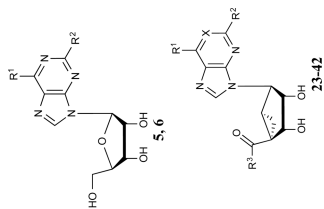




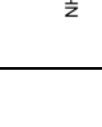
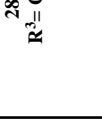


(N)-methanocarba 5'-OH derivatives

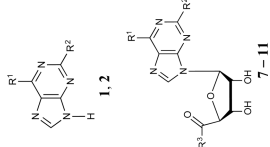
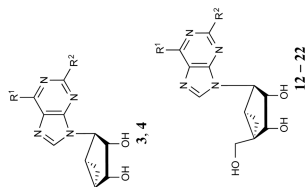
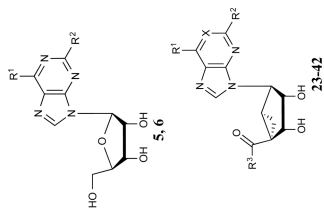
No.	R ¹	R ²	5HT _{2A} R % inhibition or K _i ^a (μM) ^d	5HT _{2B} R % inhibition or K _i ^a (μM) ^d	5HT _{2C} R % inhibition or K _i ^a (μM) ^d	A ₁ AR, % inhibition or K _i ^b (μM) ^b	A _{2A} AR, % inhibition or K _i ^b (μM) ^b	A _{2B} AR, % inhibition or K _i ^b (μM) ^b
12		Cl	<10%	>10	<10%	0.273 (r) ^c	1.91 (r) ^c	0.085 (r) ^c
13		Cl	<10%	6.47± 1.24	6.4 ^d	1.47 (r) ^c	<10% (r) ^c	0.023 ^c
14		Cl	<10%	0.0111± 0.0034	0.084± 0.024	0.039± 0.017	2.2 ^d	1.60 ±0.21
15		Cl	12%	0.476± 0.063	0.703± 0.058	0.112± 0.010	1.75± 0.19	1.2±0.4
16		Cl	<10%	0.186± 0.058	0.371± 0.043	0.076± 0.014	1.88± 0.20	0.16± 0.05
17		Cl	<10%	0.073± 0.010	0.251± 0.023	0.117± 0.010	2.95± 0.62	1.81± 0.11

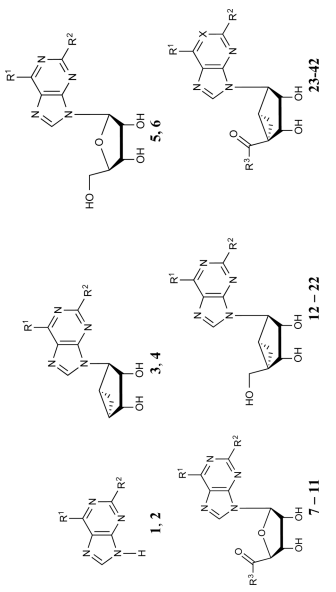
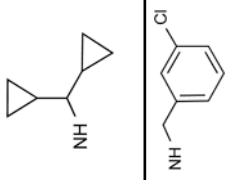
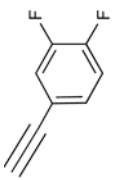
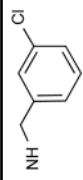
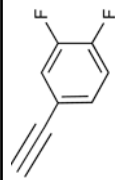
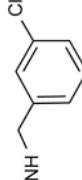
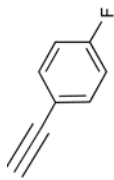
No.	R ¹	R ²	5HT _{2A} R % inhibition or K _i (μM) ^d	5HT _{2B} R % inhibition or K _i (μM) ^d	5HT _{2C} R % inhibition or K _i (μM) ^d	A ₁ AR, % inhibition or K _i (μM) ^b	A _{2A} AR, % inhibition or K _i (μM) ^b	A _{2B} AR, % inhibition or K _i (μM) ^b	
18		Cl	<10%	0.163± 0.016	0.190± 0.031	0.103± 0.007	2.20± 0.31	1.24± 0.32	
19		Cl	<10%	0.163± 0.018	0.672± 0.202	0.104± 0.006	1.52± 0.12	3.45± 0.67	
20		Cl	<10%	0.034± 0.007	0.298± 0.064	0.298± 0.004	2.69± 0.37	3.24± 0.46	
21		Cl	<10%	0.077± 0.003	0.270± 0.026	0.144± 0.032	3.94± 0.32	3.47± 0.49	
22	N(CH ₃) ₂	Cl	<10%	4.80± 0.34	8.1±0.8	11±5%	<10%	2.47± 0.44	

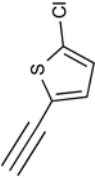
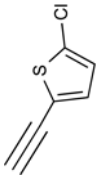
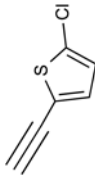
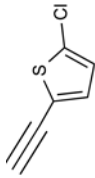
No.	R ¹	R ²	5HT _{2A} R % inhibition or K _i ^d (μM) ^d	5HT _{2B} R % inhibition or K _i ^d (μM) ^d	5HT _{2C} R % inhibition or K _i ^d (μM) ^d	A ₁ AR, % inhibition or K _i ^b (μM) ^b	A _{2A} AR, % inhibition or K _i ^b (μM) ^b	A _{2B} AR, % inhibition or K _i ^b (μM) ^b
(N)-methanocarba 5'-ester, amide and carboxylic acid derivatives								
23		Cl	<10%	0.023± 0.002	0.269± 0.007	0.110± 0.014	4.32± 0.87	0.034± 0.011
24	N(CH ₃) ₂	Cl	<10%	2.10± 0.68	4.3 ^d	26%	<10%	1.48± 0.62
25 R ³ =OCH ₃		Cl	<10%	0.019 ±0.001	0.117 ±0.011	0.437± 0.021	33%	0.766± 0.193
26 R ³ =O-CH ₂ -CH ₃		Cl	19%	0.015± 0.003	0.030± 0.002	0.360± 0.074	1.57± 0.18	0.236± 0.041
27 R ³ =O-(CH ₂) ₂ -CH ₃		Cl	<10%	0.045± 0.003	0.205± 0.073	0.440± 0.047	19±4%	0.499± 0.242



No.	R ¹	R ²	5HT _{2A} R % inhibition or K _i ^d (μM) ^d	5HT _{2B} R % inhibition or K _i ^d (μM) ^d	5HT _{2C} R % inhibition or K _i ^d (μM) ^d	A ₁ AR, % inhibition or K _i ^b (μM) ^b	A _{2A} AR, % inhibition or K _i ^b (μM) ^b	A _{2B} AR, % inhibition or K _i ^b (μM) ^b
28 R ³ = OH		Cl	<10%	1.48± 0.12	2.58± 1.34	ND	<10%	5.98± 0.30
29 R ³ = O-CH ₂ -CH ₃		Cl	<10%	0.671± 0.184	1.35± 0.19	<10%	13±6%	30±10%
30 R ³ = OH		Cl	<10%	4.70± 0.01	8.0 ^d	ND	<10%	1.08± 0.14
31 ^c R ³ =NH(CH ₂) ₂ -NH ₂		Cl	<10%	0.630± 0.146	0.142± 0.001	2.58± 1.22	23±5%	8.11± 1.27
32 ^c R ³ =NH(CH ₂) ₃ -NH ₂		Cl	<10%	1.12± 0.31	0.137± 0.019	45±4%	26±5%	55±1%
33 R ³ =NH(CH ₂) ₂ -NHAc ^c		Cl	<10%	0.332± 0.092	1.70± 0.90	0.397± 0.081	20±2%	1.65± 0.93



No.	R ¹	R ²	5HT _{2A} R % inhibition or K _i (μM) ^d	5HT _{2B} R % inhibition or K _i (μM) ^d	5HT _{2C} R % inhibition or K _i (μM) ^d	A ₁ AR, % inhibition or K _i (μM) ^b	A _{2A} AR, % inhibition or K _i (μM) ^b	A _{2B} AR, % inhibition or K _i (μM) ^b	
34 R ² =NH-(CH ₂) ₃ NH-Ac		Cl	<10%	0.534± 0.131	2.31± 0.64	46±1%	26±0%	1.97± 0.90	
35 ^c		Cl	35%	0.075± 0.007	0.168± 0.047	0.26	2.30	0.00029	
(N)-methanocarba 5'-amide derivatives with C2-arylethynyl groups									
36 ^c	NHCH ₃		11%	<10%	<10%	<10%	<10%	0.0017	
37 ^c			<10%	2.58± 0.01	7.2 ^d	<10%	41%	0.0035	
38 ^c			26%	2.12± 0.14	8.9 ^d	20%	42%	0.0022	

No.	R ¹	R ²	5HT _{2A} R % inhibition or K _i (μM) ^d	5HT _{2B} R % inhibition or K _i (μM) ^d	5HT _{2C} R % inhibition or K _i (μM) ^d	A ₁ AR, % inhibition or K _i (μM) ^β	A _{2A} AR, % inhibition or K _i (μM) ^β	A _{2B} AR, % inhibition or K _i (μM) ^β
39 ^c	NHCH ₃		19%	<10%	30%	<10%	24%	0.00070
40 ^c	NHC ₂ H ₅		<10%	13%	38%	28%	12%	0.0038
41 ^c X=CH	NHC ₂ H ₅		47%	2.21± 0.30	<10%	10%	<10%	0.0017
42	N(CH ₃) ₂		27%	<10%	8.5 ^d	25±5%	15±8%	0.0235± 0.0106

^a Binding in membranes prepared from cells stably expressing one of three 5HT₂ receptors: 5HT_{2A}R, HEK293 cells, binding with [³H]ketanserin (K_d 1.57 nM); 5HT_{2B}R, stable HEK cells, binding with [³H]lysergic acid diethylamide **43** (K_d 1.04 nM); 5HT_{2C}R, Flp IN HEK cells, binding with [³H]mesulergine **44** (K_d 2.92 nM). Values are expressed as the mean ± SEM. A percent in italics refers to inhibition of binding at 10 μM. Nonspecific binding was determined using 10 μM clozapine (5HT_{2A}R), **49** (5HT_{2B}R) or **50** (5HT_{2C}R). K_i values were calculated as reported.⁴¹ All of the compounds displayed <50% inhibition at the human 5HT_{1A}, 5HT_{1B}, 5HT_{1D}, 5HT_{1E}, 5HT₃ and 5HT_{5A}Rs, unless noted. Compound **3** bound weakly at human 5HT₃ and compound **30** bound weakly at the human 5HT_{5A}R (Supporting Information).

Author Manuscript

Author Manuscript

Author Manuscript

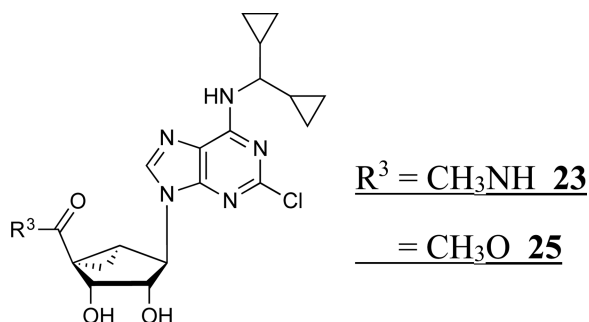
Author Manuscript

^b Affinity at the A₁AR (binding with [³H]N⁶-phenylisopropyladenosine **45**) and A₃AR (binding with [¹²⁵I]N⁶-(4-amino-3-iodobenzyl)adenosine-5'-N-methyluronamide **46**) determined as reported.^{22,24} unless noted. Selected compounds were tested for binding inhibition ([³H]2-[p-(2-carboxyethyl)phenyl-ethylamino]-5'-N-ethylcarboxamidoadenosine **47**) at hA_{2A}AR in HEK293 cell membranes. The binding affinity was expressed as K_i values (n = 2–4, unless noted). A percent in italics refers to inhibition of binding at 10 μM. Nonspecific AR binding was determined using adenosine-5'-N-ethyluronamide **48** (10 μM). Values are expressed as the mean ± SEM. K_i values were calculated as reported.⁵³

^c Archival data at ARs and 5HT₂Rs, as reported.^{22,24–27}

^d n = 1.

ND – not determined.

Table 2In vitro stability parameters for 5'-methylamide **23** and 5'-methyl ester **25**.^a

Test Compound:	23	25
Stability in simulated fluids ($t_{1/2}$, min):		
Gastric (pH 1.6)	132	125
Intestinal (pH 6.5)	>480	>480
Stability in plasma (% remaining at 120 min):		
Human	104	95.3
Rat	88.7	70.9
Mouse	95.0	61.0
CACO cell permeability:		
Papp, A->B (10^{-6} cm/sec)	4.73	18.47
Papp, B->A (10^{-6} cm/sec)	46.21	30.59
Efflux ratio	11.7	1.67
Inhibition of 5 CYP isozymes:		
IC ₅₀ , μM	>30	20 ^b
Stability in liver microsomes ($t_{1/2}$, min):		
Human ^d	130	>140
Rat	>140	>140
Mouse	>145	>140
Cytotoxicity in HepG2 cells:		
CC ₅₀ , μM	>30	>30

^aProcedures were described in Supporting Information and in Tosh et al. and Carlin et al.^{22,77}^bIC₅₀ of both compounds at the following isozymes was >30 μM (except for **25** at the 2C9, which was 20.1 μM): A2, 2C9, 2C19, 2D6, 3A4; (average of n = 2).^dCL_{int} values ($\mu\text{L}/\text{min}/\text{mg}$ protein) in human liver microsomes: **23**, 1.75; **25**, 0.77.